UCRL-10563

University of California

Ernest O. Lawrence Radiation Laboratory

TWO-WEEK LOAN COPY

This is a Library Circulating Copy which may be borrowed for two weeks. For a personal retention copy, call Tech. Info. Division, Ext. 5545

$\pi^+ - p$ SCATTERING AT 600 MeV

Berkeley, California

DISCLAIMER

This document was prepared as an account of work sponsored by the United States Government. While this document is believed to contain correct information, neither the United States Government nor any agency thereof, nor the Regents of the University of California, nor any of their employees, makes any warranty, express or implied, or assumes any legal responsibility for the accuracy, completeness, or usefulness of any information, apparatus, product, or process disclosed, or represents that its use would not infringe privately owned rights. Reference herein to any specific commercial product, process, or service by its trade name, trademark, manufacturer, or otherwise, does not necessarily constitute or imply its endorsement, recommendation, or favoring by the United States Government or any agency thereof, or the Regents of the University of California. The views and opinions of authors expressed herein do not necessarily state or reflect those of the United States Government or any agency thereof or the Regents of the University of California.

Research and Development

UCRL-10563
UC-34 Physics
TID-4500 (19th Ed.)

UNIVERSITY OF CALIFORNIA
Lawrence Radiation Laboratory
Berkeley, California

Contract No. W-7405-eng-48

π^+-p SCATTERING AT 600 MeV

Peter Cyrenius Adelbert Newcomb

(Thesis)

January 7, 1963

Reproduced by the Technical Information Division
directly from author's copy

Printed in USA. Price $2.00.
Available from the Office of Technical
Services U. S. Department of
Commerce Washington 25, D. C.

π^+-p SCATTERING AT 600 Mev

Contents

Abstract v

Introduction 1

Experimental Procedure 6

Scanning and Measuring 10

Data Reduction 12

Acceptance and Classification. 22

Corrections. 40

Normalization. 47

Results and Conclusions. 49

Acknowledgments. 71

Appendix 73

References 75

π^+-p SCATTERING AT 600 MEV

Peter C. A. Newcomb
(Thesis)

Lawrence Radiation Laboratory
University of California
Berkeley, California

January 7, 1963

ABSTRACT

The Berkeley 15-inch hydrogen bubble chamber was used at the Bevatron to investigate π^+-p interactions at 600 MeV. Seventeen hundred and thirty-eight good events were found; 71.9 ± 0.8% of these were elastic. The inelastic interactions were almost entirely single pion production.

The elastic angular distribution was fitted by a fourth order polynomial in $\cos \theta_{c.m.}$. This implies that states with an orbital angular momentum of at least 2 $\hbar$ were present. It was also shown that the upper bound of the total angular momentum was at least (5/2) $\hbar$, where $\hbar$ is Plank's constant divided by 2 π.

For the single pion production, the ratio of the number of interactions of the type $\pi^+ + p \rightarrow \pi^+ + p + \pi^o$ to those of the type $\pi^+ + p \rightarrow \pi^+ + n + \pi^+$ was found to be 5.5 ± 0.8. This result is in good qualitative agreement with the value 6.5 predicted by Sternheimer and Lindenbaum.[4] The pion momentum spectra for the reaction $\pi^+ + p \rightarrow \pi^+ + p + \pi^o$ do not show the dip predicted by Bergia, Bonsignori, and Stanghellini.[3] A peak was found in the $Q(\pi^+\pi^o)$ distribution; however, it is thought that this peak is more likely to be an effect of the (3/2, 3/2) pion-nucleon isobar than that of a π-π resonance. Angular distributions are also given for the inelastic events.

INTRODUCTION

In this experiment both elastic and inelastic π^+-p interactions were investigated in a hydrogen bubble chamber. The momentum of the incident beam was 725 ± 13 MeV/c in the laboratory. Before describing the experiment, elastic scattering and single pion production in this energy region will be discussed briefly.

Elastic Interactions

The group of reactions

$$\text{pion} + \text{nucleon} \rightarrow \text{pion} + \text{nucleon}$$

can be described by two isotopic spin amplitudes, $A_{1/2}$ and $A_{3/2}$.[1] The subscripts are equal to the total isotopic spin, T. Three of the more interesting reactions are:

$$\pi^- + p \rightarrow \pi^- + p$$
$$\pi^- + p \rightarrow \pi^0 + n$$
$$\pi^+ + p \rightarrow \pi^+ + p$$

The amplitudes for these reactions written in terms of the two isotopic spin amplitudes are respectively:

$$A^-_{el} = 2/3A_{1/2} + 1/3A_{3/2}$$
$$A^-_{ex} = \frac{\sqrt{2}}{3}(A_{1/2} - A_{3/2}) \qquad \text{(1a)}$$
$$A^+_{el} = A_{3/2}$$

The angular distribution for each reaction is proportional to the absolute square of the corresponding amplitude.

$$d\sigma^-_{el} \propto 4\left|A_{1/2}\right|^2 + \left|A_{3/2}\right|^2 + 4\mathrm{Re}A^*_{1/2}A_{3/2}$$

$$d\sigma^-_{ex} \propto 2\left|A_{1/2}\right|^2 + 2\left|A_{3/2}\right|^2 - 4\mathrm{Re}A^*_{1/2}A_{3/2}$$

$$d\sigma^+_{el} \propto \left|A_{3/2}\right|^2$$

The proportionality constant is the same if the mass difference within a given isotopic multiplet is neglected.

At 600 MeV there is a peak in the π^--p total cross section, but not in the π^+-p total cross section.[9,10] Since the π^--p system is a mixture of T = 1/2 and T = 3/2 states, while the π^+-p system is a pure T = 3/2 state, it follows that if this peak is due to a resonance, the resonance must be in the T = 1/2 state. All three of the above differential cross sections are needed to obtain $\left|A_{1/2}\right|^2$, which in turn must be fitted with phase shifts to determine whether or not one of them goes through $\pi/2$.

Another approach is to fit the π^--p and π^+-p cross section data and polarization data with phase shifts by using random search programs. The partial wave amplitudes obtained in this way are related by formulas completely analogous to (1a). The first and third of the corresponding equations for the partial waves can be solved for both the real and imaginary parts of the T = 1/2 and T = 3/2 phase shifts.[2] Thus, by using the random search technique the charge exchange data, which is difficult

to obtain experimentally, is not absolutely necessary.

For the random search method to be successful, data is required at several energies. In this experiment the elastic angular distribution, branching ratios, and numerous inelastic distributions are determined for a beam energy of 600 MeV.

Inelastic Interactions

The energy of the incident pion beam, 600 MeV, is below the threshold for the production of strange particles. Thus, pion production is the only possible inelastic process. Kinematics permits as high as triple pion production; however, from this experiment the inelastic cross section is almost entirely single pion production.

The question arises as to which of the known resonances could possibly contribute to single pion production at this energy. The reactions are:

$$\pi^+ + p \rightarrow \pi^+ + p + \pi^0$$

$$\rightarrow \pi^+ + n + \pi^+$$

There are two possibilities: either a two-pion resonance, or the (3/2, 3/2) pion-nucleon isobar. In this experiment the total mass of the two pions cannot be greater than 574 MeV. They must have $T \geq 1$ in the first reaction and $T \geq 2$ in the second. These restrictions preclude all of the established two pion resonances. This leaves the (3/2, 3/2) pion-nucleon isobar.

<u>N* (3,3) Isobar</u> This isobar has $J = 3/2$, $T = 3/2$, even parity, mass = 1238 MeV, and $\Gamma = 145$ MeV. Expanding $T = 3/2$, $T_3 = 3/2$ in terms of the isobar and one extra pion gives:

$$|\pi^+ p\rangle \rightarrow \left|\sqrt{\frac{9}{15}}\,\pi^0(\pi^+ p) - \sqrt{\frac{4}{15}}\,\pi^+(\pi^0 p) - \sqrt{\frac{2}{15}}\,\pi^+(\pi^+ n)\right\rangle$$

The brackets ( ) enclose the pair of particles forming the isobar. Thus, the isobar can contribute to both reactions being considered.

In the present experiment the pion-nucleon total mass lies between 1079 MeV and 1372 MeV. Thus, the isobar practically covers the available phase space. Therefore, the (3/2, 3/2) isobar is very likely to play an important role in single pion production in the present experiment.

Bergia, Bonsignori, and Stanghellini[3] have reformulated the isobar model of Sternheimer and Lindenbaum.[4]

The model due to Bergia <u>et al.</u>[3] (BBS) will be outlined briefly and then related to the Sternheimer and Lindenbaum model. This whole discussion follows that given by BBS.

As seen from the isotopic spin expansion above there are two amplitudes which can be formed with the isobar in the reaction $\pi^+ + p \rightarrow \pi^+ + p + \pi^0$.

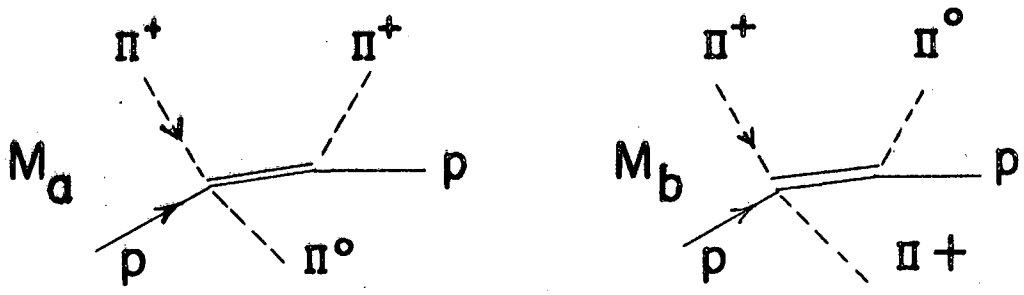

Now BBS point out that these two diagrams are indistinguishable experimentally and therefore their amplitudes should be added, not their cross sections. Thus,

$$d\sigma \sim \left| \alpha M_a + \beta M_b \right|^2 \rho$$

where α and β are the Clebsch-Gordan coefficients, and ρ is a symbol for the phase space factors. BBS used a theoretical expression for M_a and M_b which had successfully described the (3,3) elastic resonance. In order to calculate momentum spectra of the two outgoing pions, they assumed that the N^* production was isotropic and that it decayed isotropically in its own rest frame. These assumptions were made to simplify their calculations, especially since the correct production angular distribution was not known.

The interference between M_a and M_b was destructive and produced a large dip in the momentum spectra of the outgoing pions. (See Fig. 19 and Fig. 20). Now BBS state that if the interference term is neglected, their model reduces to the Sternheimer and Lindenbaum model. This corresponds to combining cross sections instead of amplitudes.

In this experiment it was of interest to see whether or not there was a dip in these momentum spectra.

In the BBS model the reaction $\pi^+ + p \rightarrow \pi^+ + n + \pi^+$ does not have an interference term, because this reaction has only one amplitude.

EXPERIMENTAL PROCEDURE

This experiment was done at the Bevatron in the Berkeley 15 inch hydrogen bubble chamber. The beam was a separated π^+ beam, which was built by G. Goldhaber, S. Goldhaber, Kadyk, Stubbs, Stork, and Ticho.[5] The layout is shown in Fig. 1. It was originally designed as a K^+ beam and was retuned to separate π^+ mesons. No change in the construction or layout of the apparatus was required. The circulating proton beam in the Bevatron was reduced to 10^9 protons per pulse in order to obtain a flux of about 25 π^+ mesons per pulse in the bubble chamber.

Goldhaber et al. have described the beam and its operation in detail. Therefore, only the changes in operating conditions required to separate pions rather than kaons will be discussed here.

As seen in Fig. 1 there were two stages of separation. This has several advantages over a long single stage as pointed out in reference 5.

To insure that the beam was centered at each of the two slits, three thin counters were mounted side by side in front of each slit. These were intended primarily to align the beam. However, even when the experiment was in progress the triad of counters at the first slit was used to keep the separated π^+ beam centered on the first slit. While the pictures were actually being taken, the pion flux was too low for the triad to give a reliable image of the beam in a single pulse, so the triad was lowered 3/4 inch into the separated proton beam. The spectrometers were well regulated which made the distance between the separated pion beam and the separated proton beam very constant. To make this distance a convenient 3/4 inch, the voltage across the

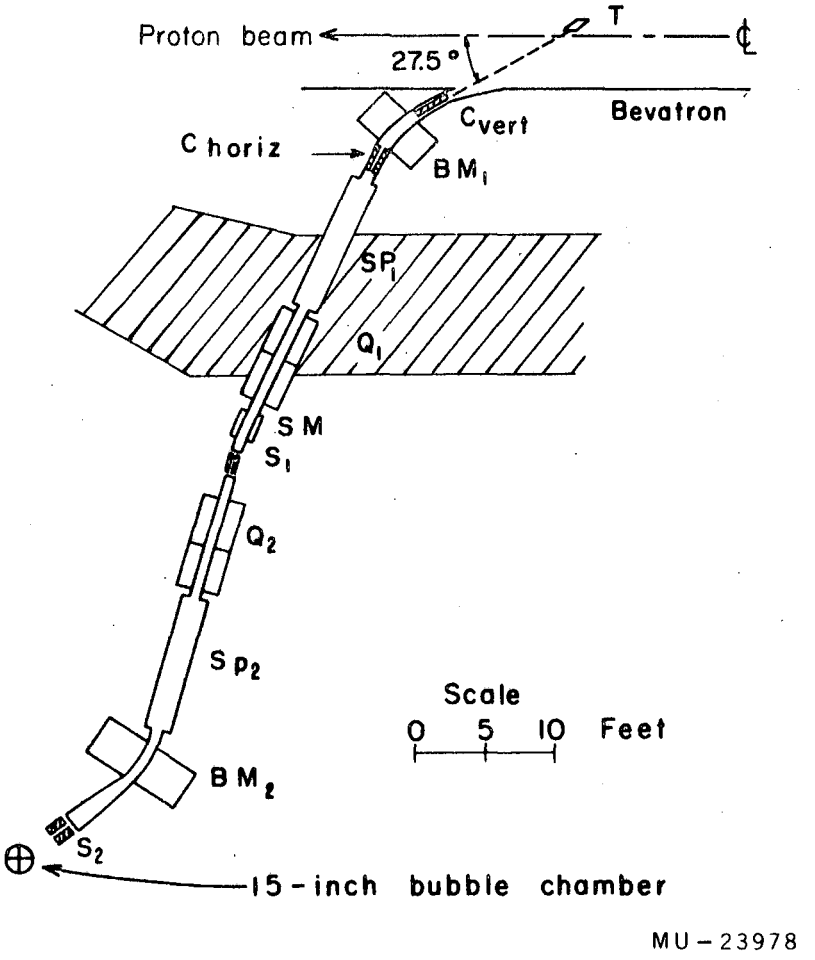

Fig. 1 Layout of the separated π^+ beam. The π^+ beam from the target (T) was focused by the quadrupole Q_1 onto slit S_1. The momentum selection was effected by bending magnet BM_1, and the subsequent mass separation by the crossed electric and magnetic fields in spectrometer SP_1. The second stage was essentially a mirror image of the first. The steering magnet SM was introduced for additional freedom in the horizontal plane. C_{horiz} and C_{vert} were horizontal and vertical collimators, respectively. (Reprinted from Phys. Rev. Letters 7, 188 (1961) by permission).

parallel plates in the first spectrometer was reduced to 164 kilovolts. The second spectrometer was operated at 310 kilovolts.

The middle counter of the second triad (B_2) and a counter on the other side of the second slit (H) were operated in coincidence to count the number of beam particles entering the chamber. This information was displayed on a pair of meters labeled B_2H, which were photographed with the bubble chamber.

The momentum was checked by stopping protons in copper directly in front of the chamber. This gave 725 ± 7 MeV/c at the center of the chamber. The quoted error is the uncertainty in the central value. In analysing the data a beam momentum of 725 MeV/c ± 1.8% at the center of the chamber was used. The 1.8% was the actual momentum spread found by Goldhaber et al.[5] The central value was also verified by curvature measurements of tracks in the bubble chamber. See Fig. 2. The errors in the curvature measurements were too large to check the spread in the beam's momentum.

The only non-negligible contamination in the beam was the μ contamination. On the basis of a comparatively crude calculation this was estimated at about ten percent. However, since no absolute cross sections were measured in this experiment, the μ contamination has no effect on the results presented.

In three and a third days of running at the Bevatron using every other pulse approximately 17,900 pictures were taken.

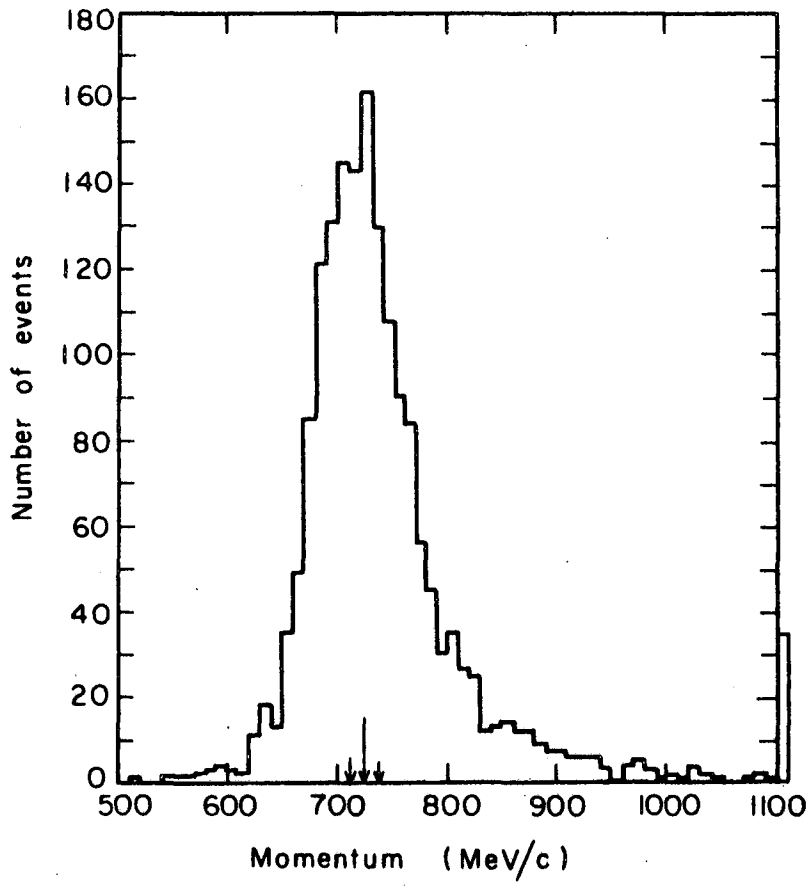

Fig. 2. Histogram of the measured momentum of the incoming pion of the 1245 elastic events and the 493 single pion production events. The arrows indicate 725 MeV/c ± 1.8%.

SCANNING AND MEASURING

In scanning the film, pictures with B_2H greater than 35 counts, or with the B_2H counter accidently turned off, were rejected. If a picture could not be scanned properly because of poor conditions in the chamber, or because the film was damaged, it was rejected. In the whole experiment 22.6% of the pictures were rejected. This included pictures which had no tracks at all; however, by far the greatest cause for rejection was too great a beam flux. ($B_2H > 35$).

A rectangular fiducial region approximately 20 cm by 20 cm was defined in one view. Defining the fiducial region in only one view was convenient for scanning, and furthermore was supplemented by much more restrictive criteria after the events were measured. The clearance between the fiducial region and the edge of the bubble chamber was about 8 centimeters at the ends and 5 centimeters on the sides.

The pictures were scanned for all interactions of beam tracks inside the fiducial region. A beam track was defined as an incoming track which (1) entered the fiducial region by crossing its upbeam edge, (2) had positive charge, (3) was within a certain projected angular interval, (4) was minimum ionizing and (5) had curvature greater than a fixed minimum.

All events, except single prong forward scatters, were submitted to be measured. There were 2494 ± 1 of these, of which all but 8 had two outgoing prongs.

The events were measured on a digitized microscope, which measured the position of points along each track with respect to fiducial marks in two views. These data were automatically punched out on IBM cards by the microscope. The punched cards were in turn used by a computer to reconstruct the events in space.

All of the scanning was done by two people, a professional scanner and the writer. There were 49 reels of film; of these 32 were scanned by the scanner and 28 by the writer. Eleven reels were scanned by both people to determine scanning efficiencies.

On the basis of the 1738 events that were eventually selected with which to do physics the average scanning efficiency for the experiment was greater than 95 percent. No scanning bias was found for the inelastic events. However, a scanning bias was observed for the elastic events. This bias was not large, and was well determined. The details of the corrections made will be explained later in the section on Corrections.

The writer looked at each event at least twice in order to find any possible errors. These were corrected during subsequent runs with the computer.

DATA REDUCTION

The data reduction of the output from the digitized microscope was done by Howard White's group using the FOG CLOUDY FAIR system of programs[6] on an IBM 7090 computer.

In very brief and much oversimplified terms the FOG CLOUDY FAIR system breaks down as follows:

FOG checks the internal consistency of the input measurements, and if these are acceptable for a given event, reconstructs positions, momenta, and angles in space. FOG also assigns the various possible combinations of masses to the tracks of each event.

CLOUDY is a kinematical analysis program. First, it calculates the errors in the measured angles and momenta, and then constrains the events to fit definite reactions. This is done by minimizing Chi-square subject to energy and momentum conservation.[6,7] The program computes the fitted quantities, their errors, Chi-square and quantities that were not measurable, such as the direction and momentum of a neutral track. Since the fitting is an iterative procedure, it also states the momentum and energy unbalance before and after iterating. CLOUDY also performs kinematical calculations such as finding momenta and angles in the center of momentum frame, etc.

FAIR provides the output format for the CLOUDY program. FAIR also makes lists and histograms of the data subject to whatever conditions the physicist requests.

A much more complete description is given in reference 6.

Preproduction

Since this was the first time FOG CLOUDY FAIR was used to analyse data from the Berkeley 15-inch hydrogen bubble chamber, it was necessary to adapt FOG to accomodate the new chamber. This was done by professional programmers in Howard White's group. The results were checked statistically by plotting scatter diagrams and histograms of a number of quantities. Among the most sensitive of these were SA, SB, and SP, each of which is defined for each track. The coordinate system is shown in Fig. 3.

The definition of SA is

$$SA \equiv \frac{\alpha_c - \alpha_m}{(\alpha_c - \alpha_m)_{rms}}$$

where α_c and α_m are the constrained and measured values of α respectively.[7] If the distribution of α_m is gaussian, then the distribution of SA is gaussian with a mean value of zero and a standard deviation of one.

SB and SP are defined in a manner completely analogous to SA. They refer to the angle β (see Fig. 3), and to the momentum respectively.

In order to use SA, SB, and SP, it is necessary to constrain the events to some hypothesis, and to select those that satisfy the hypothesis. In preproduction a portion of the events were constrained to be elastic. Those for which Chi-square was less than 13 were accepted (4 degrees of freedom). This gave samples of about 150 events. For each track of these elastic events histograms of SA, SB, and SP were plotted. By using these plots as a guide the constant associated with third order aberrations in the bubble chamber's

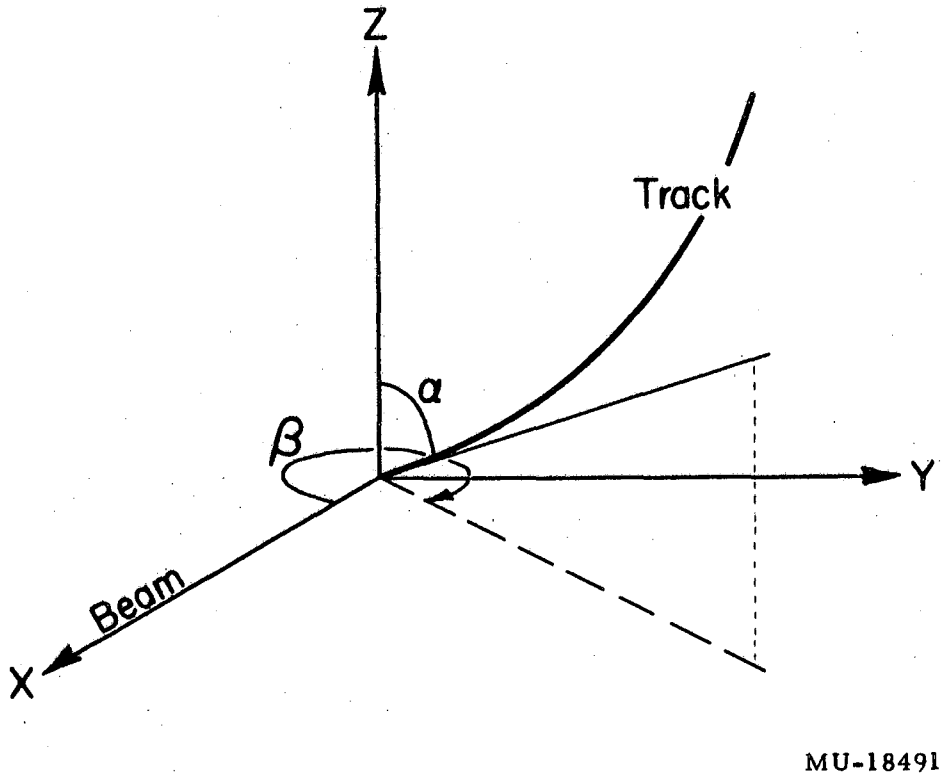

Fig. 3. The coordinate system used by FOG CLOUDY FAIR. The z-axis points towards the cameras.

optical system was evaluated. It was extremely small. Also, the value of α was adjusted 0.5 degrees. Histograms of SA, SB, and SP for each of the three tracks, after the constants in FOG were completely determined, are shown in Figs. 4, 5, and 6. These events had $\chi^2 < 13$ and also satisfied condition (4) explained in the next chapter. The histogram of SP for protons includes only those whose momenta were determined by curvature. The SP histogram for momenta determined by range has little meaning because the program fixed the measurement error on all range tracks at three percent, and would not let the constrained value of the momentum be less than the measured value. In Figs. 4, 5, and 6 the median, mean, and standard deviations are given. The normal distribution plotted on each histogram has the same standard deviation as the corresponding histogram and was centered visually for the best fit. An arrow indicates the center point. The only central value that is displaced by more than 0.2 is that for SP of the outgoing pion, which is 0.3.

The standard deviations as shown in Figs. 4 through 6 are quite close to unity; hence the errors were not adjusted in any way. Thus the errors quoted by the program were arrived at on a definite physical basis.

Beam Editing and Beam Criteria

CLOUDY substituted a value of 730 MeV/c ± 1.8% for the momentum of every beam track at a point 19 centimeters up-beam from the center of the chamber ($x = -19.0$ cm). This corresponded roughly to the end of the chamber. CLOUDY also corrected

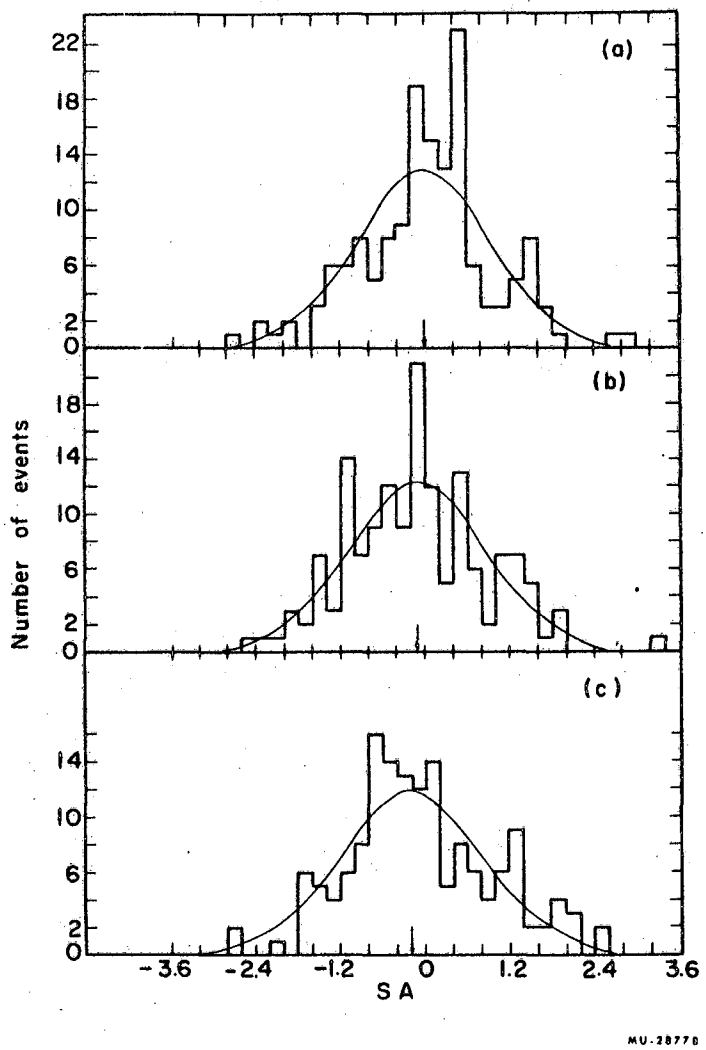

Fig. 4 (a,b,c). Preproduction. There are 152 events in each of these plots. They are histograms of SA for (a) the incoming pion, (b) the outgoing pion, (c) the outgoing proton. For each distribution the parameters are:

	median	mean	Std. Dev.	Std. Dev. of mean
(a)	0.10	0.05	0.94	0.08
(b)	-0.14	-0.13	0.98	0.08
(c)	-0.18	-0.06	1.03	0.08

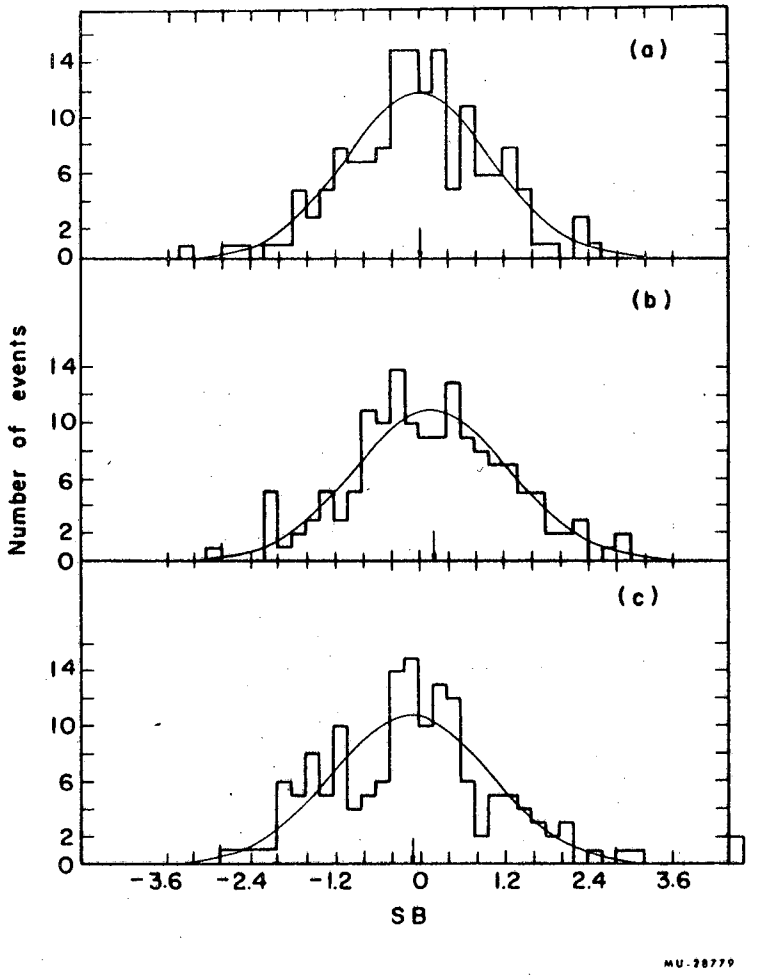

Fig. 5 (a,b,c). Preproduction. There are 152 events in each of these plots. They are histograms of SB for (a) the incoming pion, (b) the outgoing pion, (c) the outgoing proton. For each distribution the parameters are:

	median	mean	Std. Dev.	Std. Dev. of mean
(a)	-0.03	-0.02	1.02	0.08
(b)	0.15	0.16	1.11	0.09
(c)	-0.14	-0.11	1.13	0.09

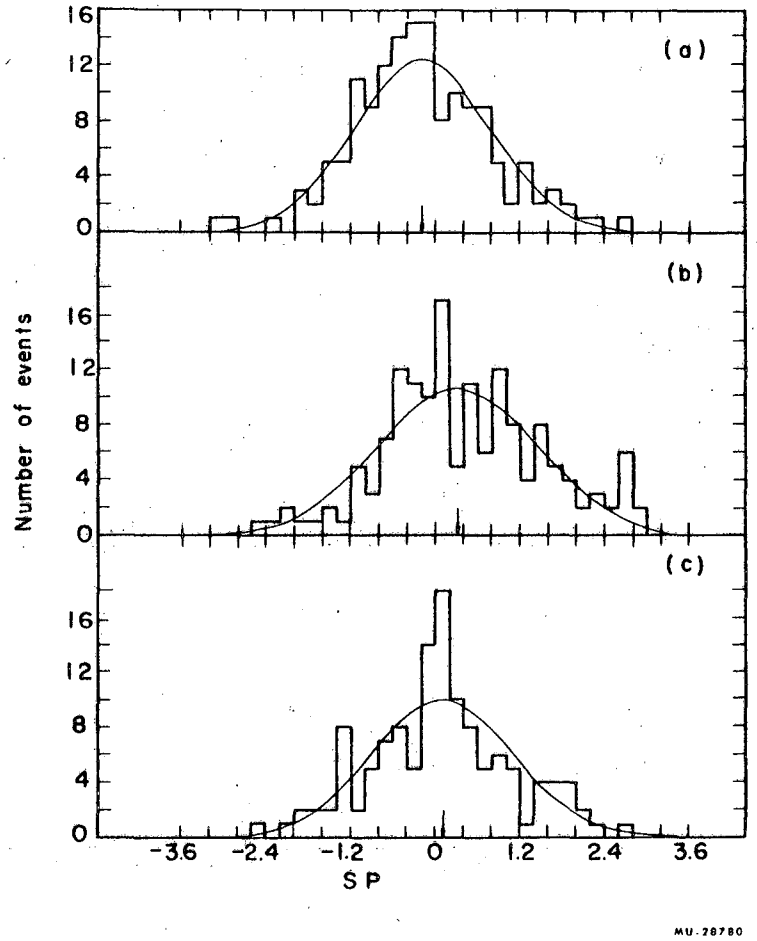

Fig. 6 (a,b,c). Preproduction. There are 152 events in (a) and (b), while there are 126 events in (c). These are histograms of SP for (a) the incoming pion, (b) the outgoing pion, (c) the outgoing proton. For each distribution the parameters are:

	median	mean	Std. Dev.	Std. Dev. of mean
(a)	-0.24	-0.17	0.98	0.08
(b)	0.30	0.42	1.15	0.09
(c)	0.04	0.07	1.01	0.09

for the energy loss in the liquid hydrogen down the beam track to the point of interaction. This corresponded to 725 MeV/c ± 1.8% at the geometrical center of the chamber.

Histograms were made of α, β, y, and z which led to the following beam criteria:

For x = -19.0 centimeters

$$\begin{aligned} 87.5^{\circ} &\leq \alpha < 93.0^{\circ} \\ 3.0^{\circ} &\leq \beta < 10.0^{\circ} \\ 63.0\text{cm} &\leq z < 68.0 \text{ cm} \end{aligned} \qquad (1)$$

There was a condition on y also; however, it merely redefined the scanning table criterion and did not eliminate any events. The median plane of the chamber in the z direction was z = 65 centimeters.

Since the elastic and inelastic π^+-p cross sections are quite strongly energy dependent in the region of this experiment, a criterion was imposed directly on the measured value of the incoming track's momentum. The criterion was

$$P_{CEN}\ (1 + DP_{EXT}) \geq 700 \text{ MeV/c} \qquad (2)$$

P_{CEN} was the measured momentum at the center of the incoming track. DP_{EXT} was the relative external error. That is, it included both the error due to multiple scattering and an expected average error made in measuring the position of the points along the track. CLOUDY also computed DP_{INT}, the internal error, which was the relative error in the momentum based on the departure of the actual measured points from the arc of a circle.

The criterion (2) was designed to eliminate pions that may have scraped the edge of the beam channel and still satisfied criteria (1). The criterion was very stringent, and it probably caused a number of perfectly good incoming tracks to be rejected. However, it was felt that it was vital that the incoming beam be very well defined, even though it reduced the statistics somewhat.

Production

The events were divided into two categories, E and N. The events in category N were obvious inelastics just from their appearance on the scan table. That is, both outgoing prongs were on the same side of the incoming track, or by comparing two views the event absolutely had to be noncoplanar, or there was a Dalitz pair (two events). Except for the two events with Dalitz pairs, all events with other than two outgoing prongs (8 events) were not processed. The events in category E then were either elastic or inelastic. CLOUDY fitted the two categories of events as follows:

Category E

$$\begin{aligned} \pi^+ + p &\rightarrow \pi^+ + p \\ &\rightarrow \pi^+ + p + \pi^o \\ &\rightarrow \pi^+ + n + \pi^+ \end{aligned}$$

Category N (3)

$$\begin{aligned} \pi^+ + p &\rightarrow \pi^+ + p + \pi^o \\ &\rightarrow \pi^+ + n + \pi^+ \end{aligned}$$

In fitting each of these reactions CLOUDY tried all possible mass permutations of the outgoing particles. Thus for category E there were five mass permutations, and for catagory N

There were three mass permutations. Only 6 events were found with more than two outgoing prongs, so multiple pion production was neglected.

The beam was edited as described in the previous section.

ACCEPTANCE AND CLASSIFICATION

The acceptance of events and their classification as elastic or inelastic was done one event at a time.

First, the measured quantities for the incoming track in the FOG CLOUDY FAIR output had to satisfy the beam criteria (1) and (2). If the incoming track of a given event did not pass the beam criteria, it was checked on the scan table. When the measure of the incoming track was at all questionable, the event was remeasured.

For each event that passed the beam criteria, the measured angles, track lengths and signs of curvature from FOG CLOUDY FAIR were checked roughly on the scan table to catch any obvious errors. The curvature was not systematically checked with templates; however, extremely obvious momentum errors were caught. If any errors were found, the event was submitted to be remeasured, unless it appeared to be unmeasurable, in which case it was rejected.

If no errors were found, the measured values of the momentum and dip angle for the two outgoing tracks were used in conjunction with the relative ionization as seen on the scan table to separate protons from pions. This was a very simple procedure. Almost all of the outgoing tracks had momenta such that if they were pions they were minimum, and if they were protons they were well above minimum, and were very dark on the scan table. In a very few cases where there was any doubt about the mass of the particle, both

possibilities were considered. It was, of course, assumed that all interactions were on hydrogen, so there could not be more than one outgoing proton. Tracks that stopped in the chamber were counted as protons. None of these showed the π-μ-e decay scheme, which would have been typical of a stopping pi-plus. Tracks that definitely went backward in the laboratory were counted as pi-pluses, because kinematics prevents the proton from doing so.

Up to this point the data for the events were checked by a professional scanner. However, the writer checked all the events that failed the beam criteria, or for which a possible error had been found at the scan table, and made the final decision on each of them.

After the mass assignment for each of the two outgoing prongs had been made, the writer made further checks on the output. The beam criteria were checked again briefly. Also, the internal consistency of DP_{INT} and DP_{EXT} was looked at. If DP_{INT} were greater than DP_{EXT} for a given track, the track was checked again on the scan table for errors in its angles or curvature. If DP_{INT} and DP_{EXT} were both greater than 10 percent, and DP_{INT} greater than twice DP_{EXT} the event was remeasured; unless a reason for the relatively large DP_{INT} could be found at the scan table, such as turbulence, or a very steep track.

Events that survived the above scrutiny were separated into elastic or single pion production catagories using Chi-square. Before going into this, it is advantageous to define four quantities that were computed by CLOUDY, F_1, F_2, F_3, and F_4. For elastic events

F_1 was the longitudinal momentum unbalance in the laboratory of all three tracks at the vertex of the event.

F_2 was the transverse momentum unbalance when all three tracks were coplanar. That is $F_2 = P_1 \sin \theta_1 - P_2 \sin \theta_2$ where P_1 and P_2 are momenta of the two outgoing tracks, and θ_1 and θ_2 are the corresponding scattering angles.

F_3 was the coplanarity $(-1 \leq F_3 \leq +1)$.

F_4 was the total energy unbalance.

For inelastic events F_1, F_2, and F_3 were the three components of the momentum unbalance. F_4 remained the total energy unbalance. The F's were evaluated by the program before and after constraining an event to fit a given hypothesis. When a neutral particle was assumed to be present then F_1, F_2 and F_3 were zero before constraints, leaving only one degree of freedom in the Chi-square sense. Elastic events had four degrees of freedom. By definition the F's had to vanish after constraints for the fitted momenta and angles to have meaning. When they did not vanish this meant that the program had been unable to fit the data to the hypothesis and that the value of Chi-square was meaningless. When the F's vanished the value of Chi-square computed by CLOUDY had meaning, and could be interpreted in terms of the Chi-square probability distribution[8]. Now, since the fitting procedure was an iterative one, the condition that the F's vanish was relaxed to that of demanding that each of the F's be less than a fixed upper limit after constraints. These were

$$\begin{aligned} |F_1| &\leq 9 \text{ MeV/c} \\ |F_2| &\leq 9 \text{ MeV/c} \\ |F_3| &\leq .009 \\ |F_4| &\leq 9 \text{ MeV} \end{aligned} \qquad (4)$$

for both elastic and inelastic events. Although these numbers were chosen somewhat arbitrarily, it was felt that they were large compared to the combined measurement errors. If after constraining an event,

the conditions (4) were not satisfied, it was said that the "fit was non-convergent". For the vast majority of those fits that did converge, all the F's were at least an order of magnitude less than their respective upper limits.

The separation was done in the following manner.

When the output for an event had been thoroughly scrutinized as previously described, Chi-square was noted subject to the condition (4) on the F's for all those hypotheses that were consistent with the previously made mass assignment and the scanning category, (E or N).

It was demanded that an event not only fit the category into which it was finally put, but further that it not fit any other permitted by the mass assignment.

The process of categorising the events one at a time was carried through three "iterations". By that it is meant that the measures were categorised; their remeasures were categorised, and the remeasures of the first remeasures were categorised. At this point over 90% of the events had been definitely categorised.

During the first two iterations even though an event could be definitely categorised as elastic (or inelastic), if its Chi-square were high, that is $\chi^2 > 15$ (or $\chi^2 > 7$), it was often remeasured on this basis alone. However, during the third iteration an event was remeasured only if there was something specific wrong with the measurement, or if there was some question about an event that had failed the beam criteria, but not on the basis of Chi-square. Further, it was made certain that no events remained to be remeasured on the basis of Chi-square from a previous iteration. Note that

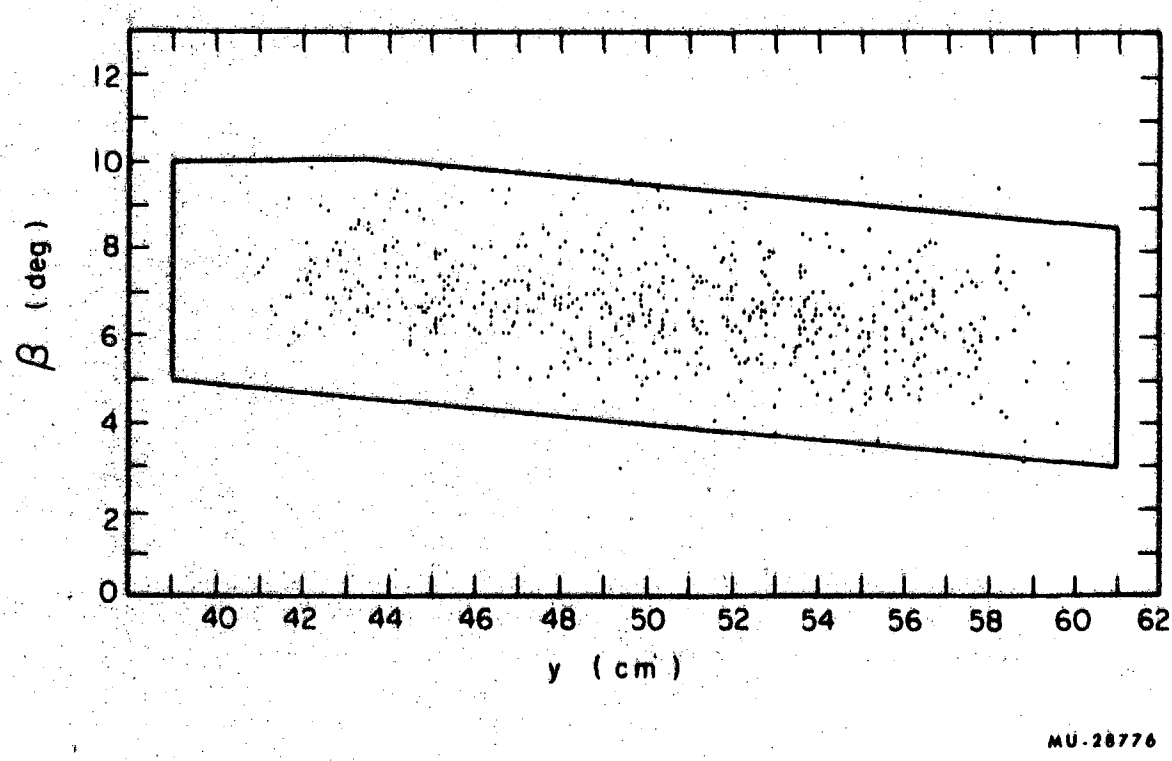

Fig. 7. β versus y for the incoming track at x = -19.0 cm. The band used as a beam criterion is outlined. The upper left hand corner is cut off because it runs into the original 10° upper bound on β. In the program the sloping lines were approximated by a series of 0.2° steps in β.

the remeasuring of events discussed above refers only to those requested by the physicist and not to those which were done automatically as a result of FOG's consistency checks.

After the events had been separated a further beam criterion was imposed. The beam was fanned out from the second slit in the x-y plane just before entering the chamber. Thus one would expect a correlation between β and y at x = -19.0 centimeters (See page 19). After the second iteration this was verified by making a scatter diagram of the measured values of β and y for about half of the elastic events. The scatter diagram showed the expected correlation, and so a band was defined. (See Fig. 7) This correlation is very consistent with that expected from the optics of the beam.[5] This was repeated for the inelastic events with the same result. Thus the band shown in Fig. 7 became an additional beam criterion that was applied to all events. This criterion was for the most part applied after separation, using the FAIR program.

The final results of the separation were as follows:

1245 events were elastic. That is χ^2 (elastic) $\leq$ 30.0, and χ^2 (1π prod) was non-convergent except for nine events where the program converged for a different, but possible, mass assignment. Of the latter nine events, five had χ^2 (1π prod) > 37.0; the remaining four had χ^2 (1π prod) 20.2, 15.5, 14.9 and 11.5. The last four events were separated by comparing elastic and inelastic Chi-squares and demanding that the constrained momenta agree with the curvature and ionization as seen on the scan table.

418 events were of the type $\pi^+ + p \rightarrow \pi^+ + p + \pi^o$. These satisfied χ^2 (1π prod) ≤ 15.0 and χ^2 (elastic) ≥ 100. For the vast majority χ^2 (elastic) > 1000. There was only one event that was permitted by the ionization to fit both $\pi^+ p \pi^o$ and $\pi^+ n \pi^+$, and for which the program converged for both possibilities. The values of Chi-square were 0.2 and 21.6 respectively.

75 events were of the type $\pi^+ + p \rightarrow \pi^+ + \pi^+ + n$. For these events χ^2 (1πprod) ≤ 15.0. There were no events in this category for which the program converged for another possible mass assignment.

49 events did not fit the elastic category or either of the single pion production categories. There was no bias in the ratio of events with outgoing protons to those without. Also no bias was found in the ratio of events in category E to those in category N. The angular distribution was plotted for the events in category E with an outgoing proton. This distribution had the same general features as the elastic angular distribution, as would be expected. It was concluded that these 49 events were unbiased, and that neglecting them would not cause a bias in the experiment. It was felt that this group of events resulted primarily from measurement difficulties, arising either in the film (small angle scatters, turbulence, etc) or in the digitized microscope. The latter was more suspect.

17 events fitted more than one category. For example, if an event had had χ^2 (1π prod) ≤ 15 and χ^2 (elastic) ≤ 100,

it would have fallen into this category. This category was checked for biases in the same way as the previous one. The angular distribution did not have quite the same general shape as the elastic angular distribution, but this difference was too small to be significant since there were so few events. Also, there were no biases in any of the ratios. Therefore, neglecting these events did not bias the experiment. The number of events in this category, as compared to the total number in the first three categories (1738 events), represents the ability to separate the three reactions. However, since these events show no significant bias there are too few of them to affect the errors in the branching ratios.

474 events failed one or more of the beam criteria. That is, they failed conditions (1) or (2), or they were not in the band shown in Fig. 7. These could not cause any bias, by definition.

150 events remained to be remeasured. Over half of these either had a definite error in the measurement of the incoming track, or else they failed the beam criteria and there was some question about the measurement. The rest of these events were tested for biases in the same way as described for the 49 events that did not fit any of the three reactions. Again, no biases of any kind were found. The events that were being remeasured because of the incoming track could not cause a bias since the incoming track is independent of the reaction.

15 events were not analysed because there was a second scatter on one of the outgoing prongs very close to the primary vertex. Since these few events would have required a separate analysis with CLOUDY, and there was no apparent bias they were neglected. These events were tested for biases in the same way as the previous three categories.

17 events were rejected because they could not be measured. This included 4 events with stopping protons too short to measure; even so, there was no apparent bias. It was not possible to plot an angular distribution for these events. However, by looking at the configuration of these events on the scan cards and the various ratios, no bias was detected.

25 events did not have sufficient output from the computer. This category was checked in the same way as the previous category. There appeared to be a small bias in the angular distribution and another in the ratio of the number of events in category E to the number in category N. However, both of these were much too small to affect the data.

8 events were not analysed because they had other than two outgoing prongs. These were made up of: 2 one-prong events which had large scattering angles compared to the usual elastic forward scatter, 4 three-prong events, and 2 four-prong events. (Two events, each with a Dalitz pair, were analysed as two-prong events and are not included here.)

These categories account for the total number of events (2493).

Finally, when the various categories that were checked for biases were combined together no significant bias could be found.

Thus, summarising the separation of the events:

$\pi^+ + p \rightarrow \pi^+ + p$	1245 events
$\pi^+ + p \rightarrow \pi^+ + p + \pi^o$	418 events
$\pi^+ + p \rightarrow \pi^+ + n + \pi^+$	75 events

and the remaining events did not cause any bias.

The Chi-square distribution for the elastic events is shown in Fig. 8. It has the general shape of the theoretical Chi-square distribution for four degrees of freedom. The peak of the experimental distribution is at about $\chi^2 = 2$, where it should be, but the tail is considerably broader than it should be. The increase in the tail of the distribution indicates that experimental errors should be increased by 20 to 25 percent which is what was expected from preproduction. The fact that the peak is in the right place even though the tail is broader than it should be indicates that the shape of the curve is somewhat distorted. This is to be expected, since some events were remeasured on the basis of Chi-square only. (See page 25).

The Chi-square distribution for the inelastic events is shown in Fig. 9. It has the same general shape as the theoretical Chi-square distribution for one degree of freedom, but it also has the same distortions that the elastic distribution has.

Chi-square is weighted according to the experimental error in the quantities used to evaluate it. Consequently, although Chi-square indicates how well a given hypothesis is satisfied, it does not give any information as to how accurately the measurements were made. In order to see the accuracy of the measurements, F_1, F_2, F_3 and F_4

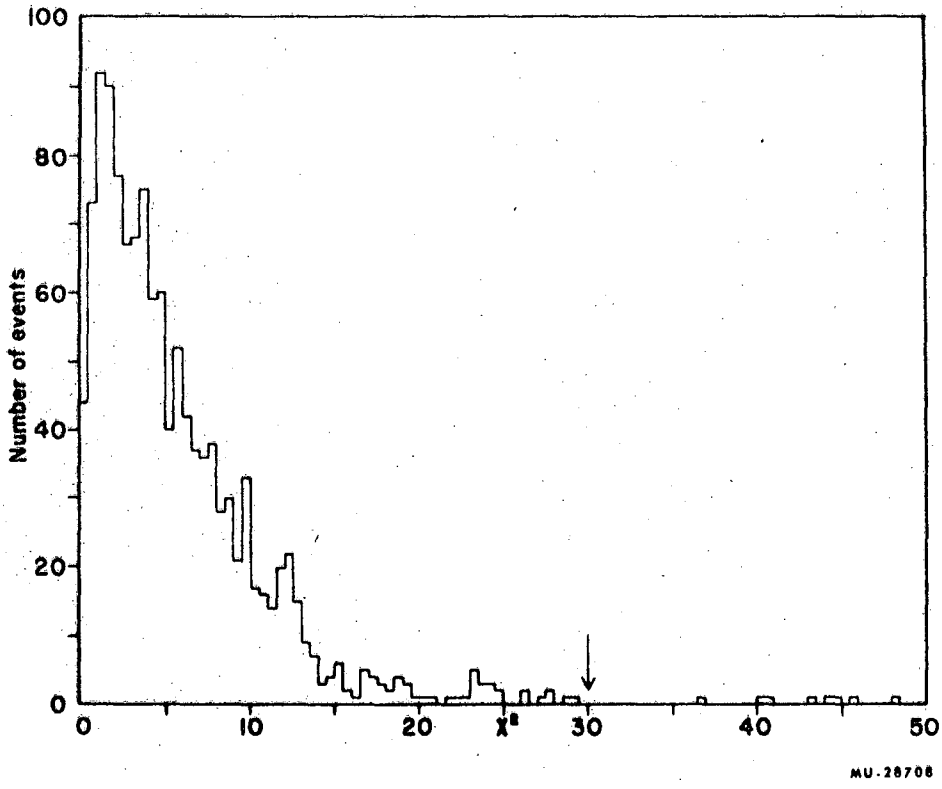

Fig. 8. Histogram of χ^2 for the elastic events. The cut off was set at $\chi^2 = 30.0$. There are 1245 events with $\chi^2 \leq 30$.

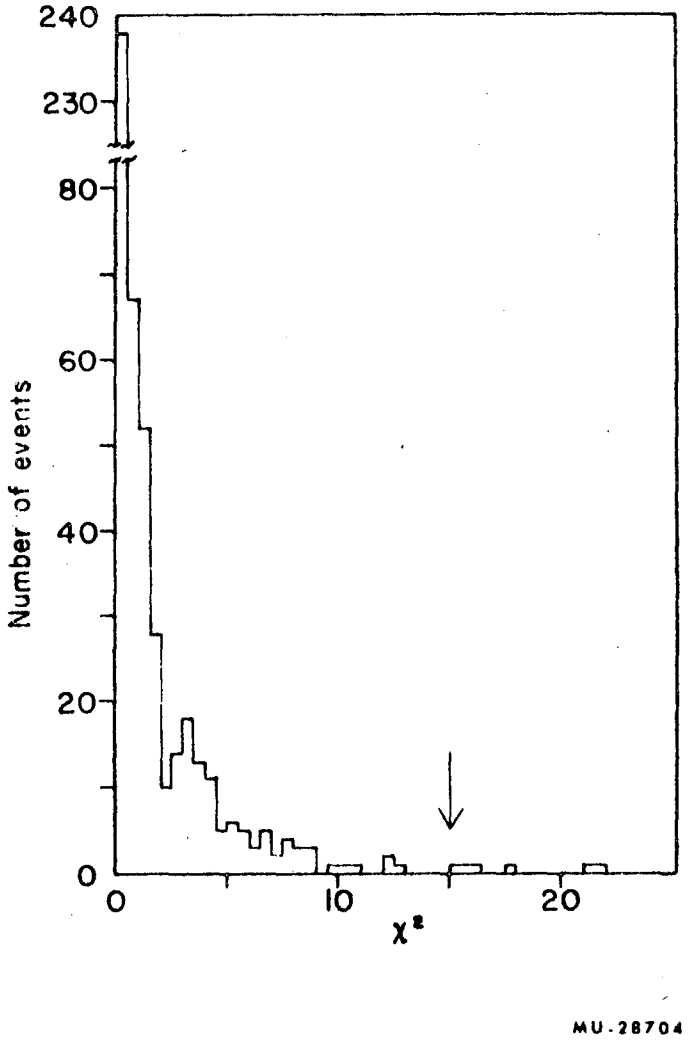

Fig. 9. Histogram of χ^2 for the inelastic events. The cut-off was set at $\chi^2 = 15.0$. There are 493 events with $\chi^2 \leq 15.0$.

evaluated before constraints are shown for the elastic events in Figs. 10 through 13. These have half-widths at half maximum of 60 MeV/c, 30 MeV/c, .010, and 60 MeV respectively. Note that the half-widths of the F's refer to the combined measurement uncertainties of all three tracks together.

The F_1 distribution is displaced to the negative side by about 20 MeV/c; there is also a corresponding displacement of about 20 MeV in F_4. This could mean that either the edited incoming momentum is high, or that the forward component of the outgoing momentum is low. It was shown on page 8 that the edited value (725 MeV/c ± 1.8%) agrees with the proton range measurement in copper and the curvature measurements of the incoming tracks made in the bubble chamber. Therefore, it is concluded that the edited beam momentum is correct within 7 Mev/c as stated on page 8, and that the displacement in the distribution of F_1, which is not large compared to the width of the distribution, is due to small systematic errors in the measurements of the outgoing tracks.

F_4 before constraints for the inelastic events is shown in Fig. 14. The half-width is 20 MeV, and there is no shift. The presence of a neutral track (i.e. one degree of freedom rather than four) makes the distribution appear more favorable than if the neutral track could actually be measured.

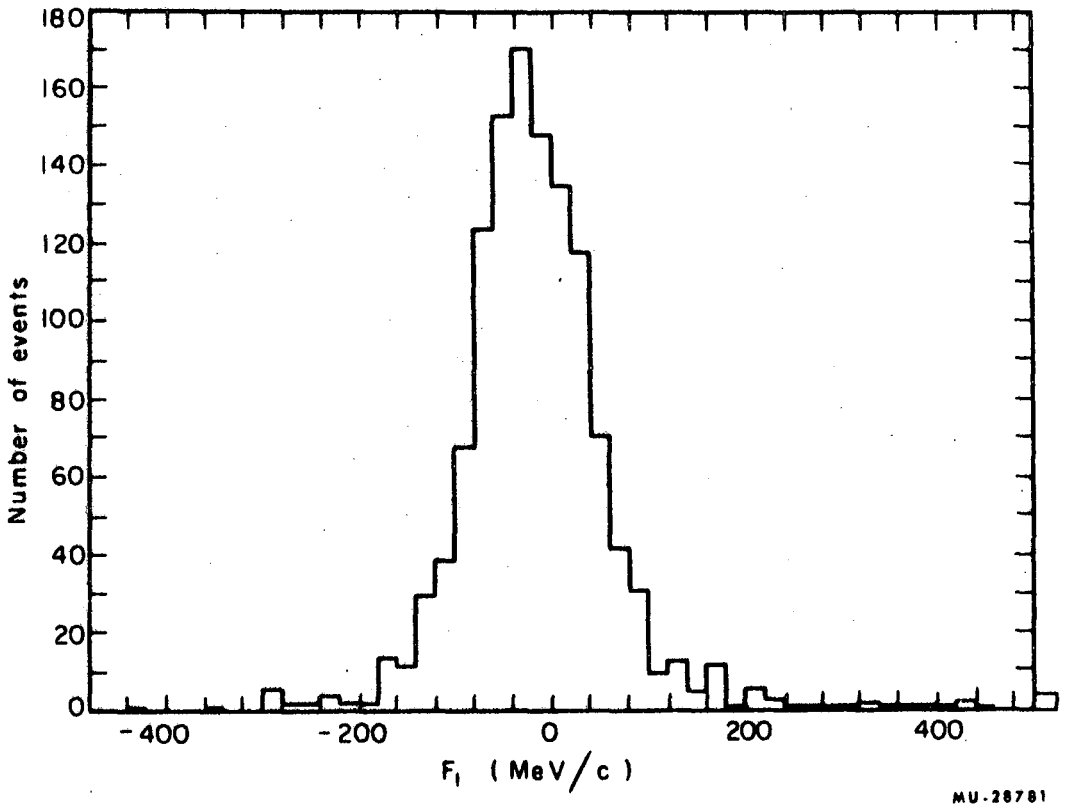

Fig. 10. Histogram of the longitudinal momentum unbalance F_1, before constraints, for the 1245 elastic events.

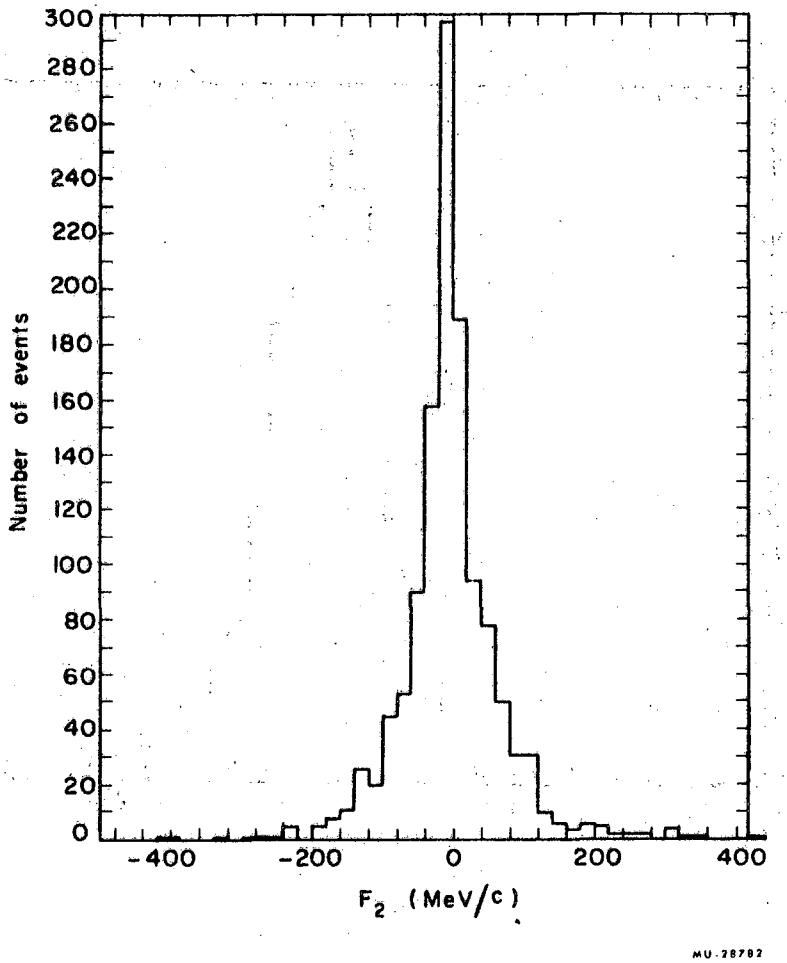

Fig. 11. Histogram of the transverse momentum unbalance F_2, before constraints, for the 1245 elastic events.

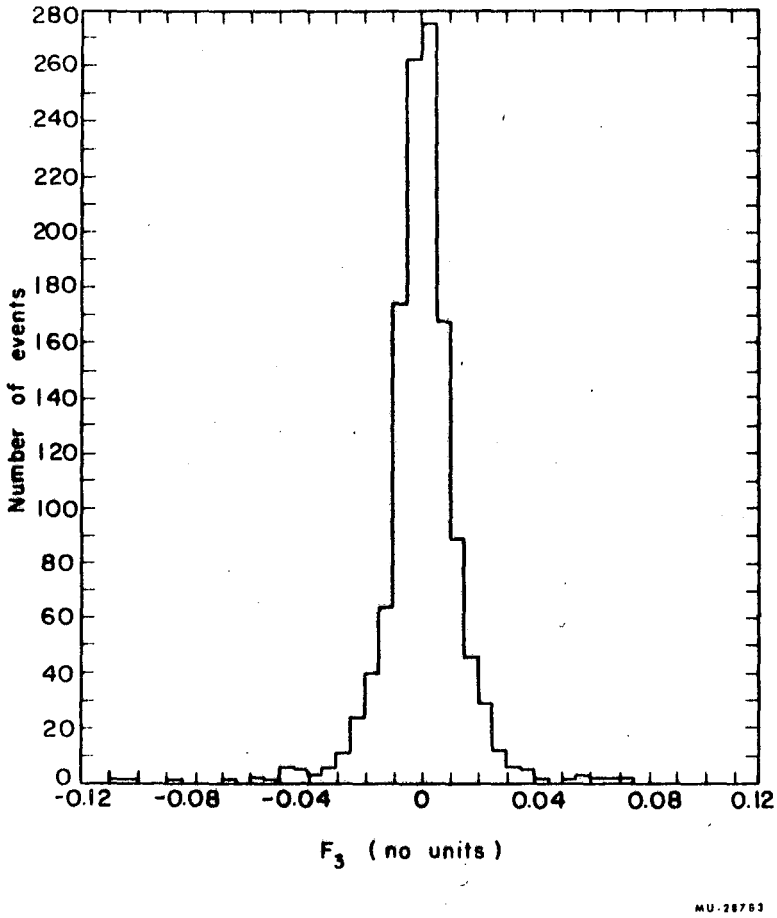

Fig. 12. Histogram of the coplanarity F_3, before constraints, for the 1245 elastic events.

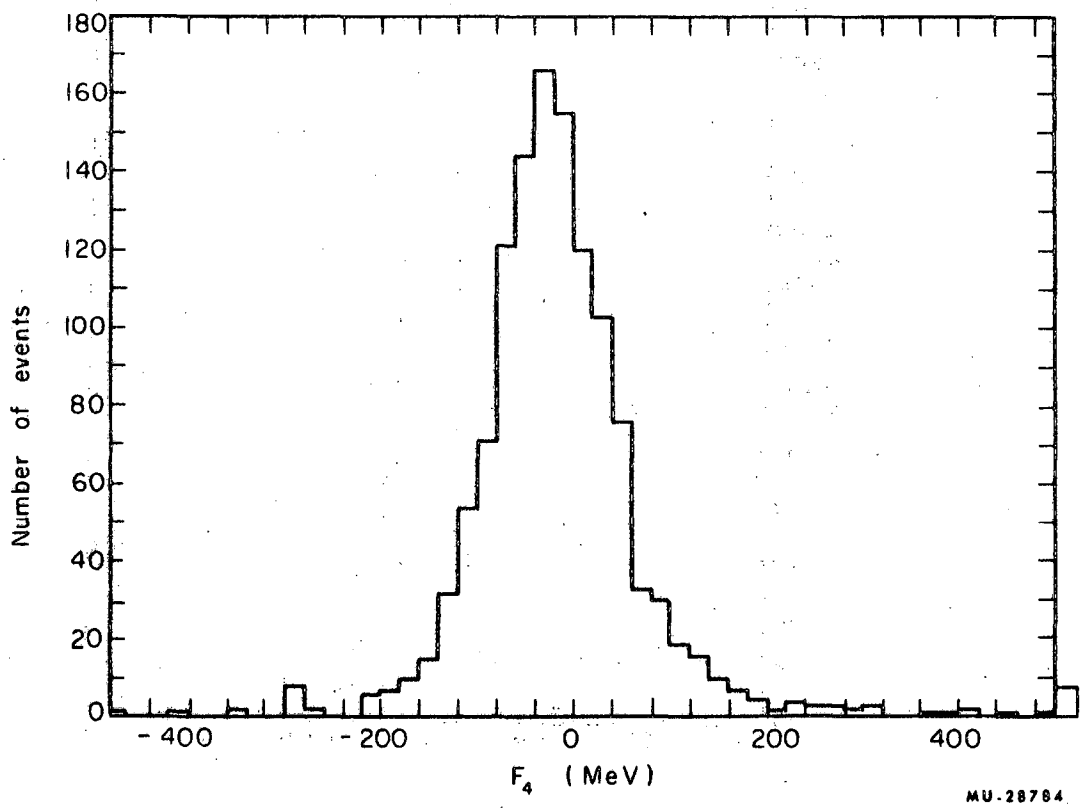

Fig. 13. Histogram of the energy unbalance F_4, before constraints, for the 1245 elastic events.

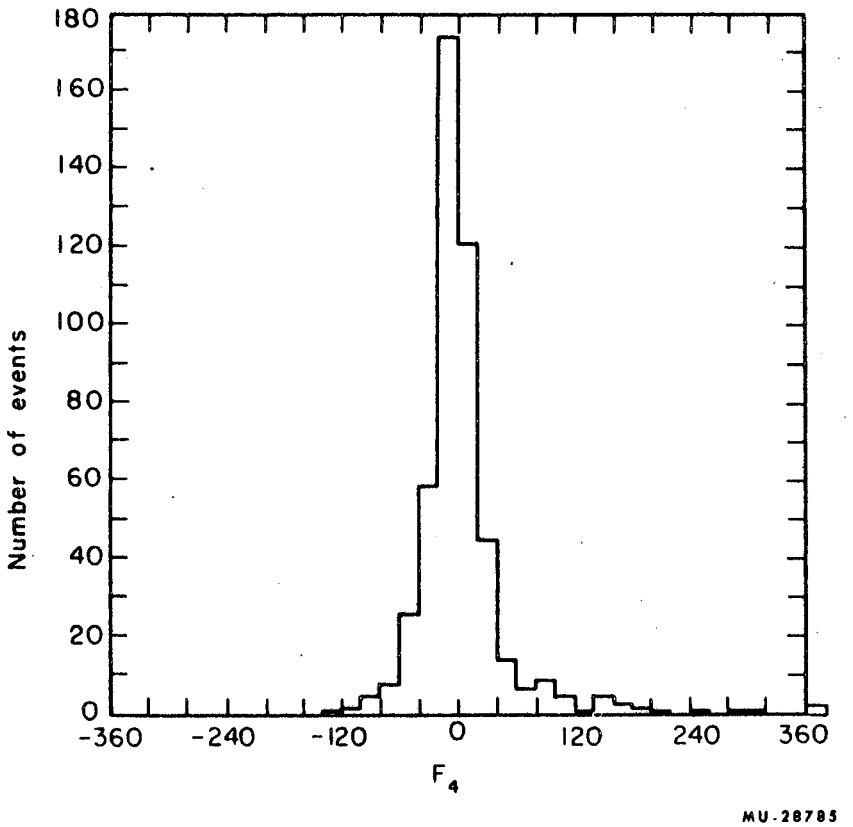

Fig. 14. Histogram of the energy unbalance F_4, before constraints, for the 493 single pion production events.

CORRECTIONS

No biases were detected as a result of the separation of the events. However, it was still necessary to correct for scanning efficiency and for any bias in the azimuthal angle, Φ. (That is, the angle between the z axis and the projection of the given outgoing track onto the plane perpendicular to the beam track. This assumes the beam track lies in a plane parallel to the x-y plane.)

The elastic and inelastic events were treated separately.

Elastic Events

The angular distribution was plotted as a function of the cosine of the pion scattering angle in the center of momentum frame ($\cos \theta_{cm}$). A cut in the forward direction was made that required $\cos \theta_{cm} \leq 0.95$. At the upper limit this corresponded to a pion scattering angle of 11.3° in the laboratory and a proton range of 0.95 cm. When projected onto the film, these correspond to: 11.3° to 1.5°, and 0.95 cm to 0.13 cm respectively, depending on the angle Φ of, say, the outgoing pion. Now, 1.5° and 0.13 cm correspond very closely to the smallest angle and track length that can be measured with the microscope. Consequently, any Φ bias should not be large for $\cos \theta_{cm} \leq 0.95$.

The angular distribution was divided into several intervals in $\cos \theta_{cm}$ and then the folded Φ distribution was plotted for each interval. These intervals were -1.0 to -0.5, -0.5 to 0.0, 0.0

to 0.5, 0.5 to 0.75, and then five intervals of 0.05 each up to 1.0. For $\cos\theta_{cm} \leq 0.85$ none of these Φ distributions showed a Φ bias. For the interval $0.85 \leq \cos\theta_{cm} \leq 0.90$ there was a small indication of a Φ bias; however, it was not statistically significant. The interval $0.90 \leq \cos\theta_{cm} \leq 0.95$ showed a definite, although not a very large Φ bias. The correction appeared to be 21 to 24 events for the 96 events that had been observed.

Out of the 49 reels of film, eleven were double scanned to determine scanning efficiencies. Two hundred and eighty four elastic events were found in the reels that were double scanned. Of these, 23 had $\cos\theta_{cm} > 0.95$, which left 261 events in the useful part of the angular distribution.

For the sake of discussion it is convenient to refer to the two scanners as A and B. Out of the above 261 events, A found one event which B had missed, while B found twelve events which A had missed. The latter twelve events were studied as a function of $\cos\theta_{cm}$ and Φ, with the result that for $0.85 \leq \cos\theta_{cm} \leq 0.95$ the scanning bias corresponded to a Φ bias, while for $\cos\theta_{cm} < 0.85$ the scanning efficiency did not depend on Φ. Therefore, for $\cos\theta_{cm} < 0.85$ the usual random scanning efficiency and correction to the data was calculated for each column in $\cos\theta_{cm}$. Only three columns had efficiencies of less than 100% and required corrections, and even these were small. (See Fig. 18.) For $0.85 \leq \cos\theta_{cm} \leq 0.95$ each of the two columns was corrected for Φ bias. These corrections were 6 events and 21 events. (See Fig. 15) These corrections were actually made on the basis of the Φ distributions broken down according to scanner, as well as for the data collectively.

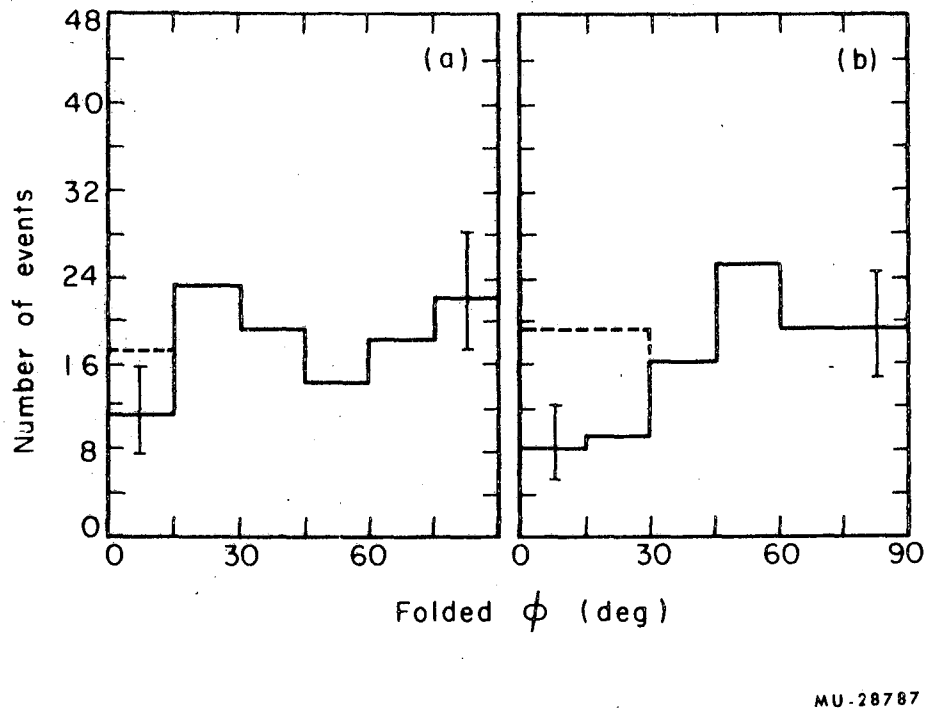

Fig. 15 (a,b). Histograms of the folded Φ distribution for the elastic events with cos $\theta_{c.m.}$ intervals (a) $0.85 \leq \cos\theta_{c.m.} \leq 0.90$ (107 events observed) and (b) $0.90 \leq \cos\theta_{c.m.} \leq 0.95$ (96 events observed). The solid lines are the observed data. The dashed lines show the corrections. Folded $\Phi = 0^{\circ}$ lies in the plane perpendicular to the film plane.

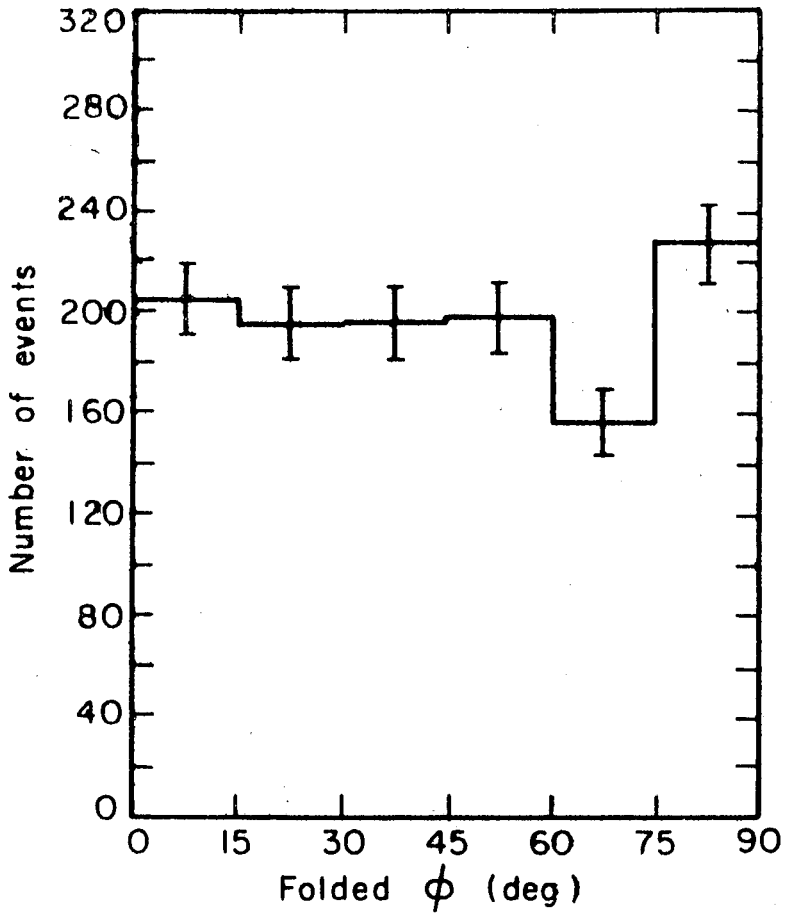

MU-28786

Fig. 16. Histogram of the folded Φ distribution for 1179 observed elastic events with $\cos \theta_{c.m.} \leq 0.95$. Folded $\Phi = 0^{o}$ lies in the plane perpendicular to the film plane.

In all of the above corrections the error was taken as the square root of the correction. Since these corrections were for systematic effects, the error in each was added linearly (not in quadrature) to the error in the original data to which the correction had been applied.

The folded Φ distribution, before corrections, for all of the elastic events for which $\cos \theta_{cm} \leq 0.95$ is shown in Fig. 16.

(P + 0) Events

Even though the incoming and the two visible outgoing tracks are not necessarily coplanar, the Φ distribution of any outgoing particle should be isotropic. Thus, even though the test is not as significant as for elastic events, where an actual correction can be made for Φ bias; distributions both in Φ, and in folded Φ, of the outgoing π^+ for various scattering angles of the π^+ were made. All of these were isotropic. Possibly a more significant test was the Φ distribution, and the folded Φ distribution, of the π^+ for all those (P + 0) events where the proton stopped in the hydrogen and had a range of less than two centimeters. There were only six such events in all, and they were randomly distributed in Φ and in folded Φ. Thus, no biases were found by looking at the 418 (P + 0) events as a whole. In the film that was double scanned 80 (P + 0) events were found. Of these, one was found by scanner A and missed by scanner B, while five were found by B and missed by A. By looking at sketches of these five events, no particular configuration was found. Furthermore, the scattering angle distribution, and the folded Φ distribution, of the outgoing π^+ for these five events were completely random.

Of these five events only two had stopping protons, and both of these had ranges greater than or equal to five centimeters. Thus, no scanning biases were found.

It was concluded that there were no significant biases in the 418 (P + 0) events. Therefore, the scanning efficiency was calculated assuming randomness, and the total number of events was corrected for the purpose of estimating branching ratios. This correction was 14 events, making the total number of (P + 0) events 432 ± 25. The error is $\sqrt{418} + \sqrt{14}$.

It is thought that the reason a Φ bias was seen for the elastic events, but not for the (P + 0) events, is that elastic scattering includes a diffraction peak which contains a sizeable fraction of events which are hard to see, while single pion production has no such peak.

(n + +) Events

The two charged outgoing particles were identical, so Φ distributions were of little use in looking for biases. However, the positive pions did not stop in the chamber; therefore, all of the (n + +) events had outgoing tracks that were long enough to be readily visible on the scanning table. Furthermore, they did not have to be coplanar as in the case of elastic events. Thus, the factors which frequently contribute to an azimuthal bias were not present.

In the film that was double scanned, 23 (n + +) events were found. Scanner A did not find any events which scanner B missed, but scanner B found three events which scanner A missed. The

three events showed no special configuration, so scanning efficiencies were calculated assuming randomness, and the correction to the total number of (n + +) events was found. The correction was 4 events, which made a total of 79 ± 11 (n + +) events. The error is $\sqrt{75} + \sqrt{4}$.

NORMALIZATION

No attempt was made to measure the total path length of the incident pions in this experiment. Instead, existing total cross section measurements were used to normalize the data.

Two extensive counter experiments to measure the π^+ - p total cross section as a function of energy have been done in the last three or four years. One was done by Brisson et al.[9] at Saclay and the other by Devlin et al.[10] at Berkeley. In the energy region of the present experiment there appears to be a systematic difference in the two total cross section measurements. Using the fitted curves, this difference is 2.6 mb at 600 Mev., which is slightly larger than the sum of the errors from the two experiments. At one energy this difference would not be too surprising, but here it persists as a function of energy. At the present time the writer knows of no explanation for the difference in the two experiments. Consequently, the choice of one total cross section experiment over the other is, to a considerable extent, arbitrary.

The present experiment has been normalized to the results of Brisson et al.[9] The reasons for the choice were: (1) the Brisson data was more consistent with the earlier experiments;[11] (2) normalizing the present experiment to the Brisson result leads to a total elastic cross section which is more consistent with the result of Helland et al.[12]

Fitting a smooth curve to the data of Brisson *et al.*[9] gives

$$\sigma_{total}(\pi^+ - p) = 16.1 \pm 0.8 \text{ mb.}$$

at a kinetic energy of 600 Mev for the incident pion in the laboratory.

RESULTS AND CONCLUSIONS

Elastic Events

The angular distribution after being corrected, as explained in the section on Corrections, was fitted to a polynomial in cos $\theta_{c.m.}$

$$\frac{d\sigma}{d\Omega} = \sum_{k=0}^{n} a_k \cos^k \Theta_{c.m.}$$

The least squares fitting was done by an IBM 704 program, PALSI,[13] for all values of n in the interval $1 \leq n \leq 10$. There were twenty experimental points, which are listed in Table I. The errors in the original data were taken as the square root of the number of events, except when there were fewer than 25 events. In the latter case one half of the difference between the upper and lower limits of the 68.3% confidence interval, as determined from the Poisson distribution, was used.[14] For numbers above 25 this is very nearly $\sqrt{N}$. As explained in the section on Corrections, when a correction was added to a column its error and the error in the original data were added linearly.

The Chi-square of the fit divided by the number of degrees of freedom is plotted as a function of n, the order of the polynomial, in Fig. 17. From this figure it is seen that the angular distribution is properly fitted by a fourth order polynomial. The angular distribution is shown in Fig. 18.

Integrating the area under the fitted curve in Fig. 18 gives

Table I. The experimental data for the elastic angular distribution.

Interval in cos $\theta_{c.m.}$	Number of events observed	Correction	Final number of events	Uncertainty (events)
-1.0 to -0.9	5		5	2.77
-0.9 to -0.8	8		8	3.35
-0.8 to -0.7	11		11	3.84
-0.7 to -0.6	9		9	3.52
-0.6 to -0.5	9		9	3.52
-0.5 to -0.4	0		0	0.92
-0.4 to -0.3	4		4	2.53
-0.3 to -0.2	8		8	3.35
-0.2 to -0.1	10		10	3.68
-0.1 to 0	14		14	4.26
0 to 0.1	27		27	5.20
0.1 to 0.2	41		41	6.40
0.2 to 0.3	62		62	7.87
0.3 to 0.4	66		66	8.12
0.4 to 0.5	128	3	131	13.04
0.5 to 0.6	144		144	12.00
0.6 to 0.7	157	1	158	13.53
0.7 to 0.8	179	8	187	16.21
0.8 to 0.9	201	6	207	16.63
0.9 to 0.95	96	21	117x2	14.38x2

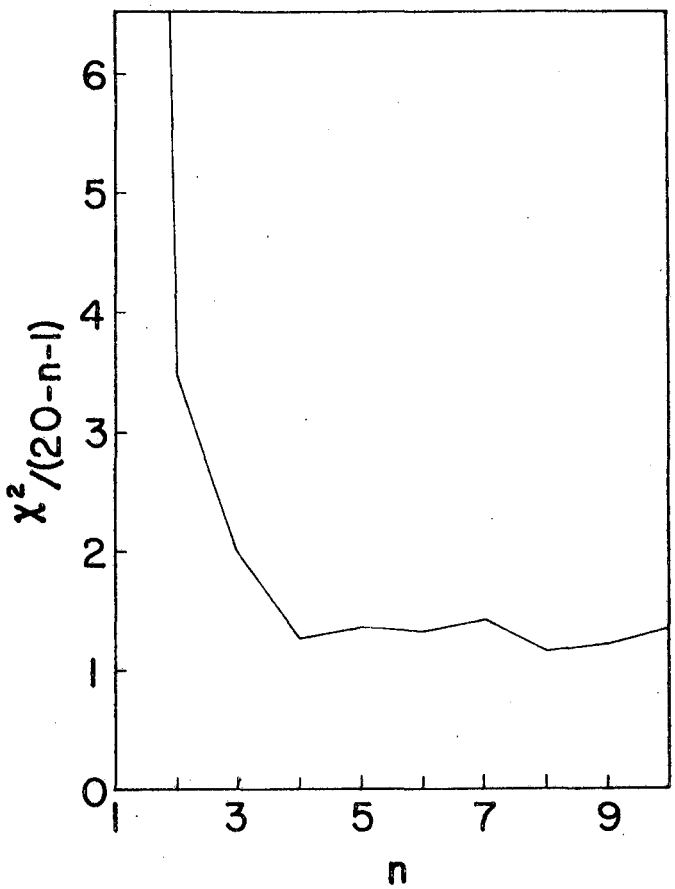

MU-28707

Fig. 17. Chi-square divided by the number of degrees of freedom for the least squares fit of the polynomial in cos $\theta_{c.m.}$ to the elastic angular distribution, plotted as a function of the order, n, of the polynomial.

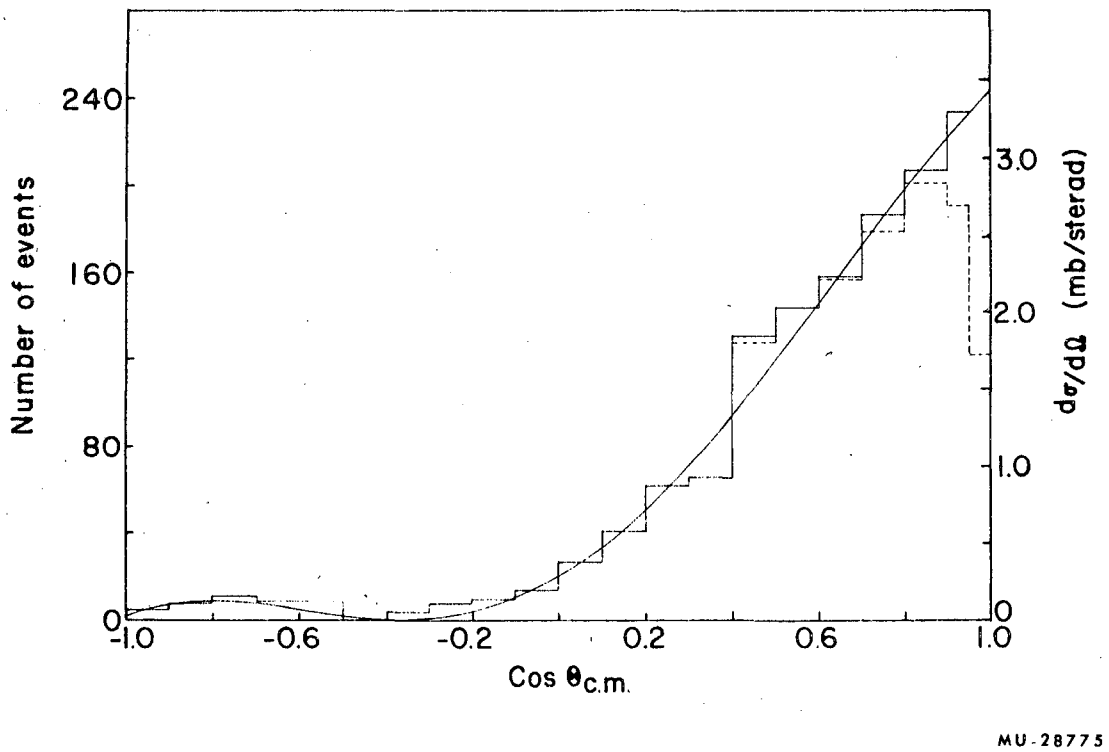

Fig. 18. The angular distribution of the elastic events. The smooth curve is that of the least squares fitted polynomial $\sum_{k=0}^{4} a_k \cos^k \theta_{c.m.}$ It is fitted to the solid line histogram which runs from -1 to 0.95. (See Table I.) The dotted line histogram shows the data before any corrections were made. The resolution of $\cos \theta_{c.m.}$ is less than half of the cell width used in the histogram.

1310 ± 14 elastic events. The error is that due to fitting; it is smaller than $\sqrt{1310}$ because it has been assumed that a fourth order polynomial in cos $\theta_{c.m.}$ fits the shape of the distribution. Using this number of elastics along with the corrected number of (P + 0) and (n + +) events given in the section on Corrections, the data was normalized to σ_{Total} = 16.1 ± 0.8 mb. This gave

$$\sigma_{elastic} = 11.6 \pm 0.6 \text{ mb}$$

Table II gives the coefficients of the fitted polynomial in cos $\theta_{c.m.}$. The uncertainties given in this table include both the fitting error, and the error due to normalization. The two relative errors were combined in quadrature according to the method of propagation of errors. Table III gives the error matrix for the coefficients. Although this matrix has been normalized, it contains only the fitting error; it does not include the uncertainty due to normalization.

Dispersion Relations From the fitted curve the differential cross section in the forward direction is

$$\frac{d\sigma\ (1)}{d\Omega_{cm}} = 3.43 \pm 0.35 \text{ mb/sterad,} \qquad \text{Experiment}$$

where the error includes both the uncertainty due to fitting as well as that due to normalization.

By using Cronin's evaluation of the real part of the forward scattering amplitude from dispersion relations[15] together with the optical theorem, the differential cross section in the forward direction was calculated.

$$\frac{d\sigma\ (1)}{d\Omega_{cm}} = 2.92 \pm 0.42 \text{ mb/sterad} \qquad \text{Dispersion Relations}$$

Table II. The coefficients of the polynomial in cos $\theta_{c.m.}$ fitted to the elastic angular distribution. The errors include the uncertainty due to normalization.

a_0 mb/sterad	a_1 mb/sterad	a_2 mb/sterad	a_3 mb/sterad	a_4 mb/sterad
0.30 ± 0.03	1.64 ± 0.14	2.53 ± 0.25	0.06 ± 0.22	-1.09 ± 0.31

Table III. The error matrix for the coefficients of the polynomial in cos $\theta_{c.m.}$ fitted to the elastic angular distribution. Although this matrix is normalized, it contains only the fitting error; it does not include the uncertainty due to normalization.

	0	1	2	3	4
0	$.0008 \left(\frac{\text{mb}}{\text{sterad}}\right)^2$	.0010	-.0025	-.0018	.0013
1		.0108	.0138	-.0192	-.0247
2			.0458	-.0206	-.0562
3				.0490	.0547
4					.0945

The main contribution comes from the real part of the forward scattering amplitude. It was also responsible for most of the error. The error in the real part was taken to be ten percent. This may be small, since at this energy the $\pi^- - p$ total cross section is going through a peak.

The dispersion relation result is apparently quite consistent with the experimental result.

Discussion of Coefficients From Table II it is seen that the largest coefficients are a_1 and a_2. This is to be expected, since the energy of this experiment is still in the region of the (3/2, 3/2) resonance.

Since $\cos^4\theta_{c.m.}$ is required to fit the data, at least D wave must be present. If one terminates the partial wave expansion at D wave, the coefficient of $\cos^4\theta_{c.m.}$ is

$$\frac{45}{4k^2}\left\{|A_2^+|^2 + 4\,\mathrm{Re}\,A_2^- A_2^{+*}\right\}$$

where

$$A_2^{\pm} = \frac{e^{2i\delta^{J=\ell\pm 1/2}_{\ell=2}} - 1}{2i}$$

and δ is the complex phase shift. (See Appendix.) Since experimentally this coefficient is negative, it follows that both A_2^+ and A_2^- must be non-zero. Therefore, at least J = 5/2 contributes to the angular distribution.

The experimental value of the coefficient a_3 is small, and quite consistent with zero. However, even when the series is terminated at $D_{5/2}$, four amplitudes contribute to a_3. This makes any simple direct inference impossible.

Comparison with other experiments† It was pointed out in the section on Normalization that one of the reasons for normalizing to Brisson's[9] total cross section was that it gave a total elastic cross section that was more consistent with Helland's result at 582 MeV.[12] The total elastic cross sections are, in fact, in excellent agreement. However, the important point is that each of the five coefficients in the $\cos \theta_{c.m.}$ polynomial is also in very good agreement.

A hydrogen bubble chamber experiment was done by W. J. Willis[16] at 500 MeV in which he found 228 elastic scatterings. The elastic cross section varies too rapidly with energy to compare that experiment directly to the present one. However, Helland has measured the elastic differential cross section at 533 MeV, and these results appear to be in quite good agreement with those of Willis, especially in view of Willis' comparatively low statistics. Other bubble chamber measurements of the π^+ - p elastic differential cross section have been made, but these were done at considerably higher energies.[17] The one nearest to this experiment is at 820 MeV.[18]

Branching Ratios

Using the numbers of events already presented and the total cross section interpolated from the Brisson data, the branching ratios and cross sections were calculated. These are shown in Table IV. The estimated errors are one standard deviation. The errors in the cross section include the error due to normalization.

Since the possibility of biases in this experiment has been investigated very carefully, as described earlier, it is felt that the results obtained for the branching ratios are accurate within the stated errors.

---

†See Note on page 61.

Table IV. Branching ratios and cross sections.

Reaction	No. of events observed	No. of events after corrections	Branching ratio (%)	Cross Section (mb)
$\pi^+ + p \rightarrow \pi^+ + p$	1245	1310 ± 14	71.9 ± 0.8	11.6 ± 0.6
$\pi^+ + p + \pi^0$	418	432 ± 25	23.7 ± 1.4	3.8 ± 0.3
$\pi^+ + n + \pi^+$	75	79 ± 11	4.3 ± 0.6	0.7 ± 0.1
all other	6 [a]		$\lesssim 1.$	$\lesssim 0.2$

[a]Six events out of 2494 had more than two outgoing charged prongs. (See text.)

The multiple pion production branching ratio was crudely estimated as follows. Six events out of 2494 had more than two outgoing tracks (2 four-pronged events and 4 three-pronged events). These six events represent one of three possible channels for double pion production. Thus, 6 (3)/2494 = 0.007. This indicates multiple pion production is $\lesssim$ 1%, since there was no evidence of more than two pions ever being produced.

In this energy region the branching ratios are changing quite rapidly with energy. There is no existing data to which the branching ratios determined in this experiment can be meaningfully compared.† The only meaningful check, which has already been discussed, was for the elastic events.

Inelastic Events

From this experiment the ratio of (P + 0) to (n + +) events was found to be:

$$(P + 0)/(n + +) = 5.5 \pm 0.8$$

Sternheimer and Lindenbaum predict a value of 6.5 for this ratio.[4] The value Willis found is $1.5_{-0.5}^{+1.5}$ at a beam energy of 500 MeV.[16] This suggests that as the beam energy increases from 500 MeV to 600 MeV the relative contribution of the isobar increases quite considerably.

(P + 0) Events The momentum spectra for the outgoing π^+ and for the outgoing π^0 are shown in Figs. 19 and 20, respectively; phase space and the curves for both isobar models are also shown. All curves are normalized to the area of the corresponding histogram. Neither the π^+ nor the π^0 spectrum shows the dip predicted by BBS.[3] Qualitatively, the histograms appear to be made up partly of phase space

† See Note on page 61.

and partly of the Sternheimer and Lindenbaum model. However, this may also mean the assumptions made by BBS regarding the angular distributions for the production and decay of the isobar were too crude. (See Introduction.)

The Q-value between the π^+ and the π^0 is shown in Fig. 21. There is a definite peak in the histogram, centered at 210 MeV. The dashed curve represents a simple Breit-Wigner formula for a pion nucleon resonance with a mass of 1238 MeV and a width of 145 MeV.[19] It was felt that this would be an adequate approximation of the Sternheimer and Lindenbaum model to compare to the experimental π-π Q-value distribution.

The three possible Dalitz plots were made of the 418 (P + 0) events. (Not shown.) These plots showed the very broad maxima of the pion-nucleon isobar. However, they did not indicate that there was a π-π resonance. Also, the distribution of the opening angle between the two pions shown in Fig. 23 follows phase space quite closely. Therefore, it is not likely that the 210 MeV peak in Fig. 21 (mass = 486 MeV) is a π-π resonance; however, this possibility cannot be ruled out.

The angular distribution for each of the three outgoing particles is shown in Fig. 22. The reason for the difference between the angular distributions of the two pions may be that the π^+ comes from the decay of the isobar more frequently than does the π^0.

<u>(n + +) Events</u> The momentum spectra of both outgoing pions are shown added together in Fig. 24. The dashed curve represents an approximation of the Sternheimer and Lindenbaum model. It was calculated in a manner analogous to that explained in the previous subsection. The histogram in Fig. 24 appears to follow phase space; however, there are only 75 (n + +) events, which are not enough to

show the shape of the distribution accurately.

The Q-value distribution for the two π^+ mesons is shown in Fig. 25. Here again, there are too few events to determine the shape of the distribution. Phase space and the simplified isobar model calculation give very similar curves. It is noted that the results of Stonehill and Kraybill[20] for this same distribution appear to follow phase space. Their beam energies were 910 MeV, 1090 MeV, and 1260 MeV.

The angular distributions of the outgoing particles are shown in Fig. 26. The distribution of the opening angle between the two pions is shown in Fig. 27. These are very similar to the corresponding distributions for (P + 0) events.

Summary

The elastic angular distribution (Fig. 18) was fitted by a fourth order polynomial in $\cos \theta_{c.m.}$ (Table II). Therefore, at least D-wave must have been present. It was also shown that at least $J = 5/2$ was present. (Appendix).

The branching ratios and partial cross sections are given in Table IV. The inelastic cross section is almost entirely single pion production.

The ratio (P + 0)/ (n + +) was found to be 5.5 ± 0.8. The prediction of Sternheimer and Lindenbaum for this ratio is 6.5.[4]

The pion momentum spectra for the 418 (P + 0) events (Figs. 19 and 20) do not show the dip predicted by BBS.[3] They are in qualitative agreement with the isobar model of Sternheimer and Lindenbaum. There is a peak in the $Q(\pi^+\pi^0)$ distribution. (Fig. 21).

The inelastic data (in particular the (P + 0) events) appear to be dominated by the (3/2, 3/2) isobar, and are qualitatively described by the Sternheimer and Lindenbaum model, (that is, the BBS model without the interference term.) The detailed shapes of the momentum spectra, however, and the peak in the $Q(\pi^+\pi^0)$ distribution, remain unexplained. Since the isobar model curve for $Q(\pi^+\pi^0)$ in Fig. 21 represents an approximate calculation, and since its maximum lies directly under the peak, possibly a more precise calculation would explain the peak.

It would be interesting to see the effect of requiring in the BBS model that the isobar decay in the $P_{3/2}$ state.†

Note

There is an unpublished preliminary report by Berloutaud et al.[21] on π^+-p scattering in a hydrogen bubble chamber at 600 MeV. The preliminary data of Barloutaud et al.[21] appear, on the whole, to agree with the present experiment. There were, however, two points about which there is some difference. (1) A third order polynomial in $\cos\theta_{c.m.}$ was sufficient to fit their elastic angular distribution, but they make the comment that this may be due to their limited statistics (339 elastic events). (2) Their result for the ratio (P + 0)/(n + +), 4.6 ± 1.1, is statistically in agreement with the result of the present experiment, 5.5 ± 0.8, but is quite far from the prediction of Sternheimer and Lindenbaum.[4]

Their results for the pion momentum spectra in the reaction $\pi^+ + p \rightarrow \pi^+ + p + \pi^0$ agree very well with the present experiment (Figs. 19 and 20).

† This effect is included in the recent model of Olsson and Yodh. See M. Olsson and G. B. Yodh, University of Maryland, Department of Physics and Astronomy Technical Report No. 293; P. Newcomb, Lawrence Radiation Laboratory Report UCRL-10682.

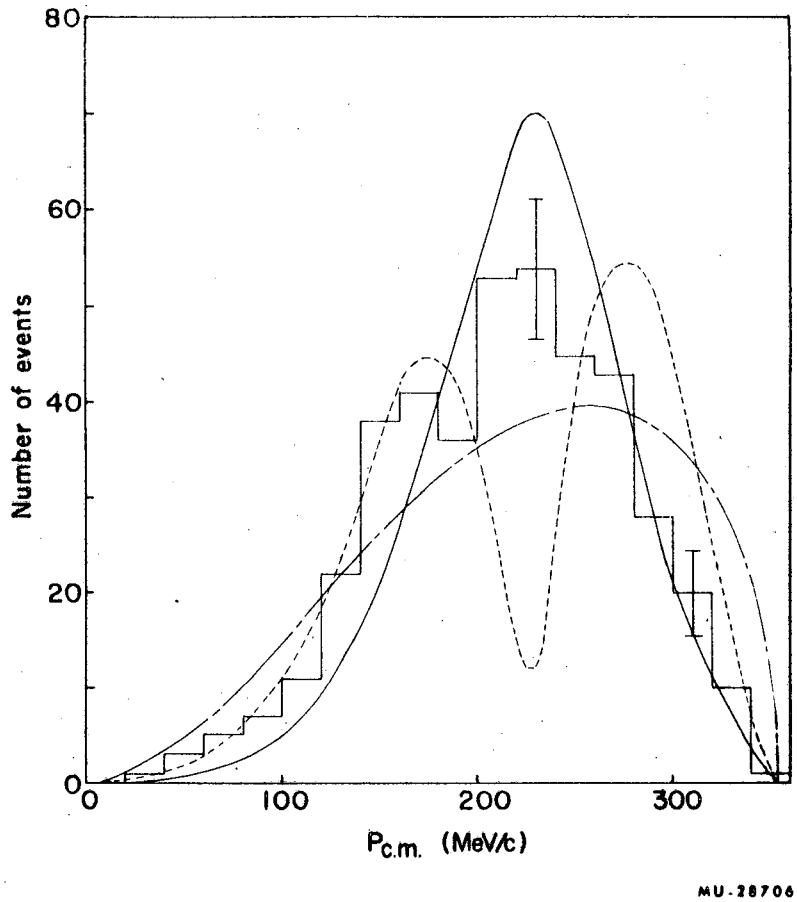

Fig. 19. The momentum spectrum of the π^+ for the 418 inelastic (P + 0) events. The solid line represents the isobar model without interference, and the dashed line the isobar model with interference. The dot dash line is invariant phase space. All three curves are normalized to the same area as the histogram. The two isobar model curves were taken from reference 3.

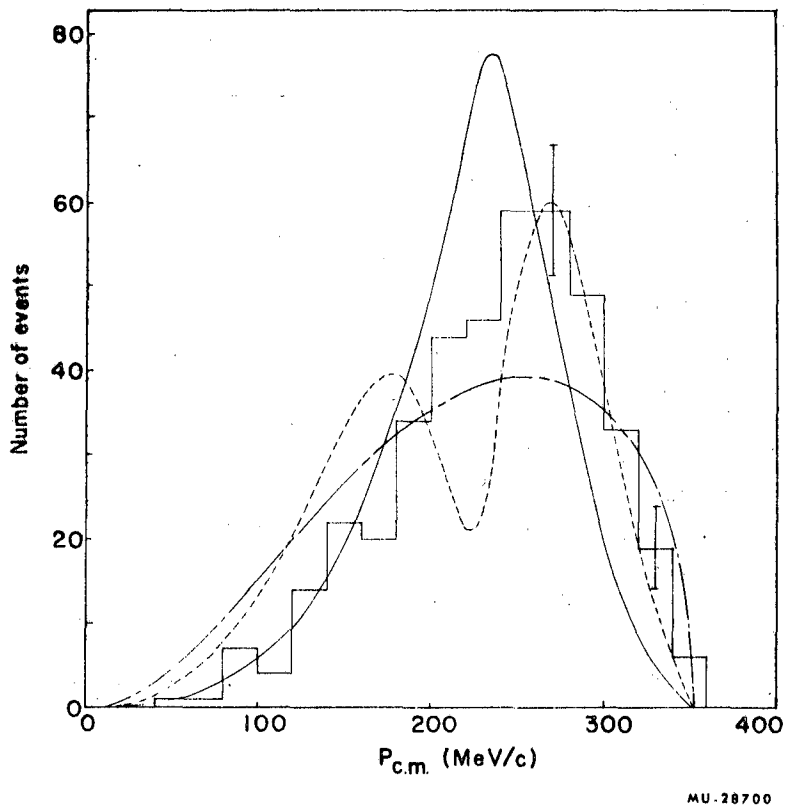

Fig. 20. The momentum spectrum of the π^0 for the 418 inelastic (P + 0) events. The solid line represents the isobar model without interference, and the dashed line represents the isobar model with interference. The dot dash line is invariant phase space. All three curves are normalized to the same area as the histogram. The two isobar model curves were taken from referemce 3.

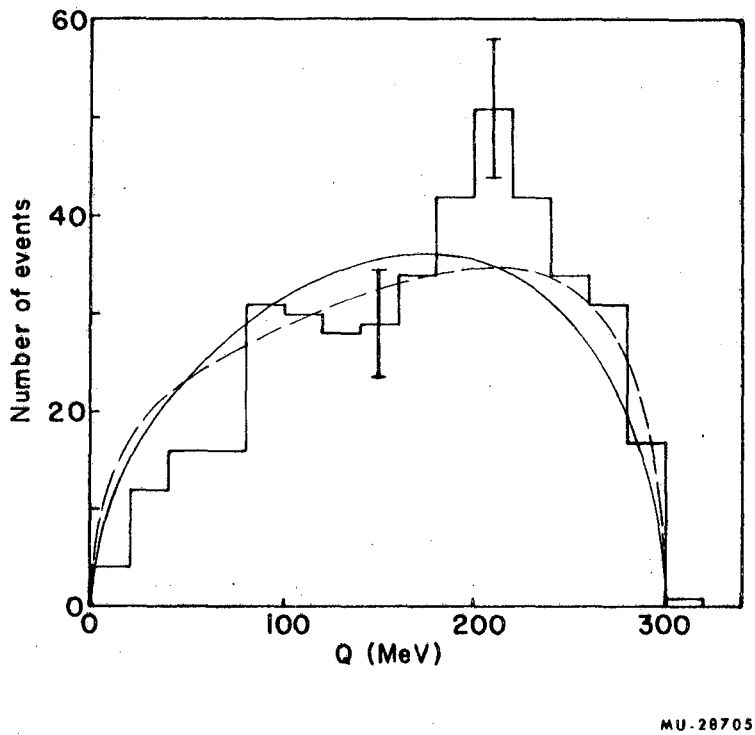

Fig. 21. Distribution of the Q-value between the π^+ and the π^0 for the 418 (P + 0) events. The solid line is phase space. The dashed line represents a simplified isobar calculation. All curves are normalized to equal area.

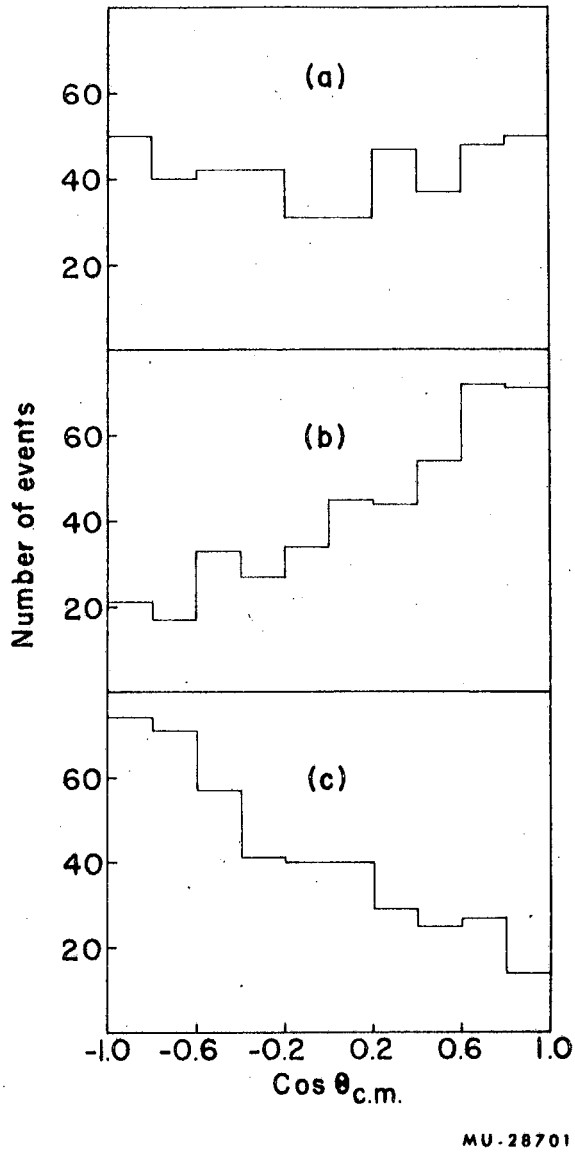

Fig. 22 (a,b,c). Distribution of the cosine of the center of momentum scattering angle of (a) the π^+, (b) the π^0, (c) the proton for the 418 (P + 0) events.

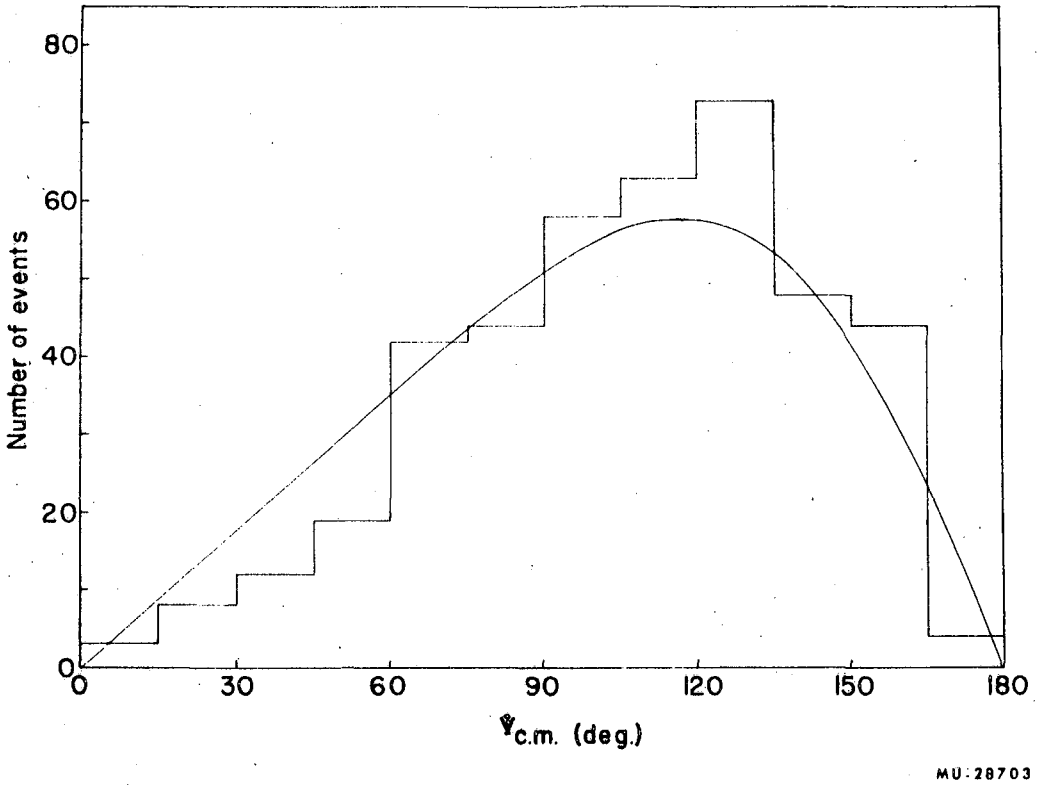

Fig. 23. Distribution of the opening angle between the π^+ and the π^0 in the reaction's center of momentum frame for the 418 (P + 0) events. The solid curve is phase space.

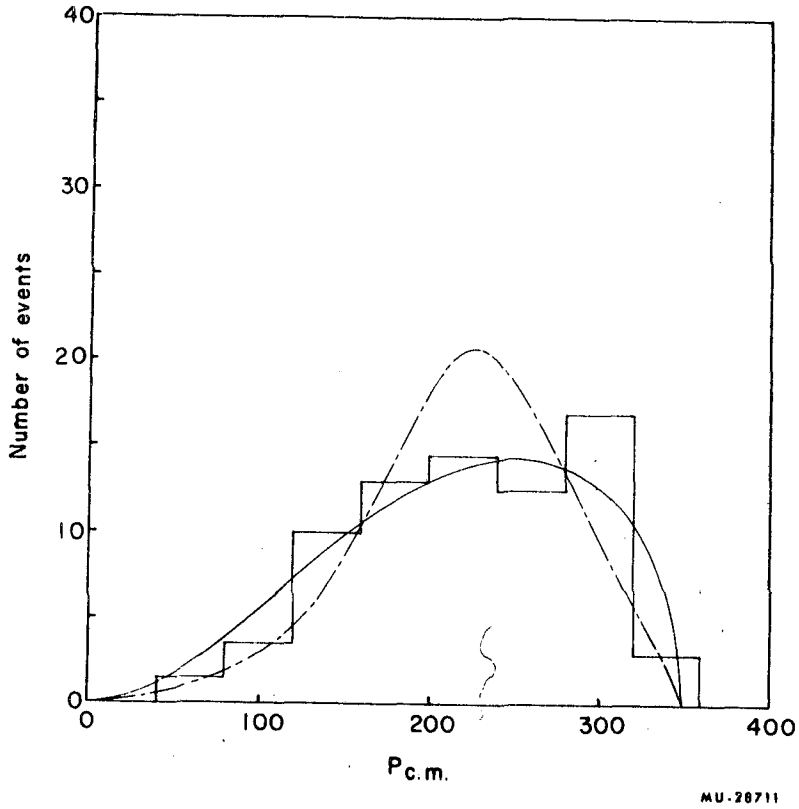

Fig. 24. The combined momentum spectra of the two π^+ mesons for the 75 (n++) events. Thus, there are 150 points in this histogram. The solid curve is phase space. The dashed curve represents a simplified isobar model calculation.

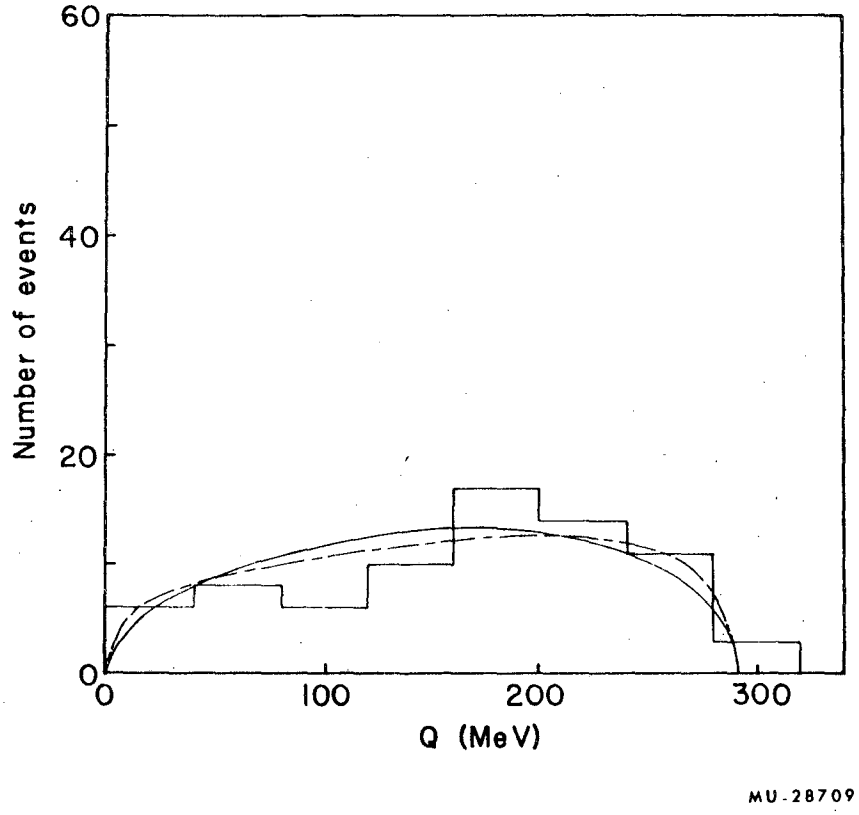

Fig. 25. Q-value distribution of the two π^+ mesons for the 75 (n + +) events. The solid curve is phase space. The dashed curve represents a simplified isobar model calculation.

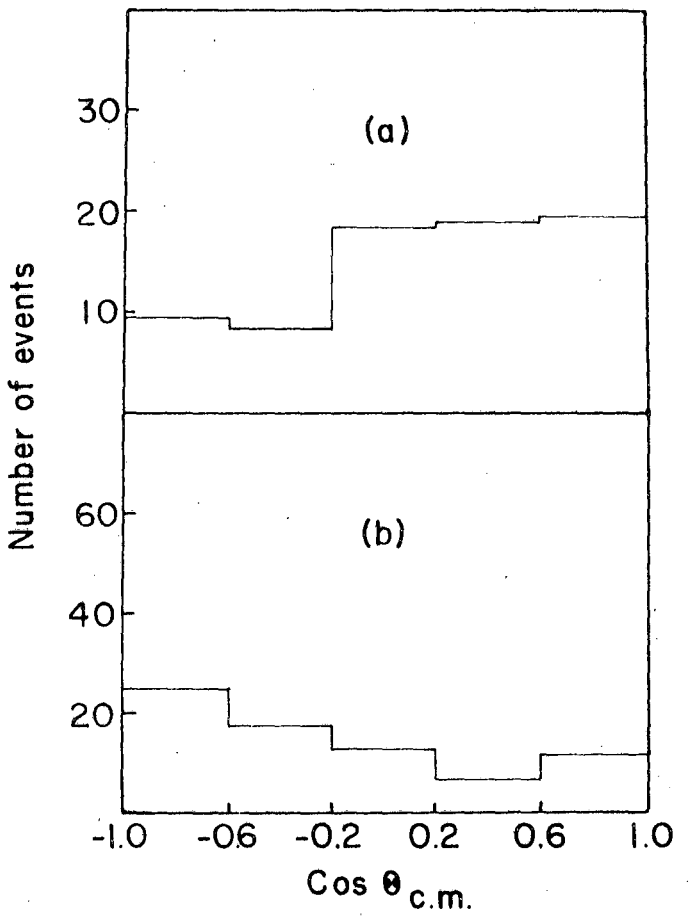

MU-28710

Fig. 26 (a,b). Histogram of the cosine of the center of momentum scattering angle of (a) the two outgoing π^+ mesons, (b) the outgoing neutron for the 75 (n + +) events. There are 150 points in (a) and 75 points in (b).

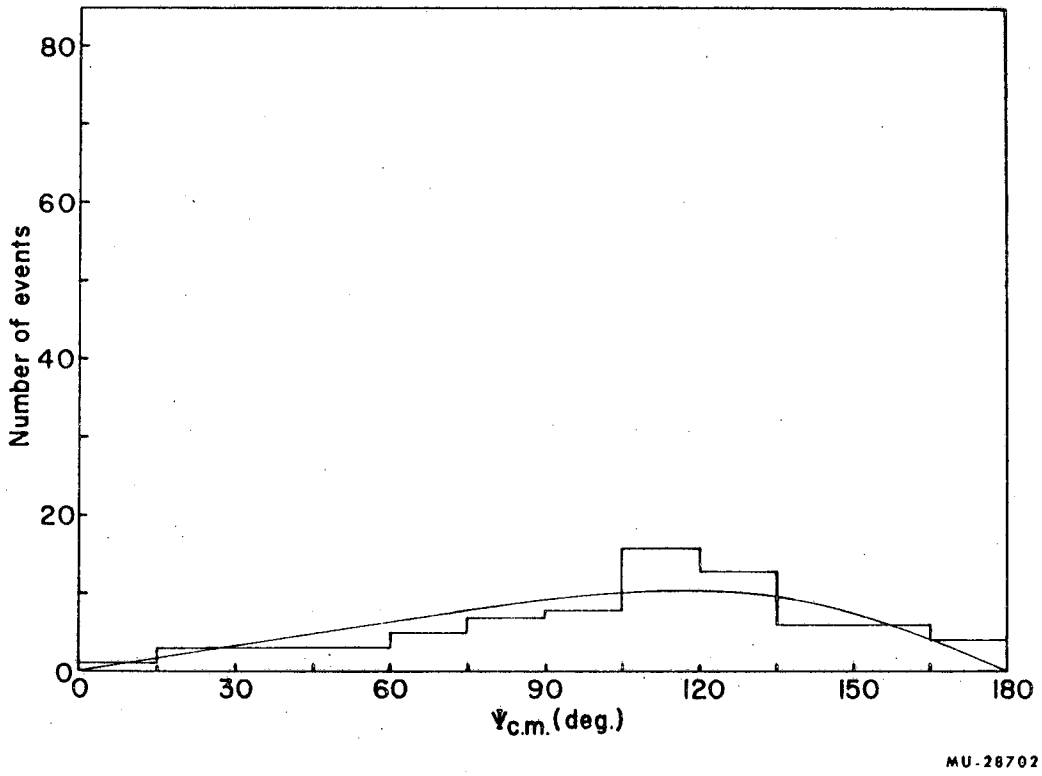

Fig. 27. Distribution of the opening angle between the two π^+ mesons in the reaction's center of momentum frame for the 75 (n + +) events. The solid curve is phase space.

ACKNOWLEDGEMENTS

I would like to thank Professor Wilson M. Powell for the patience and guidance he has shown me during my years as a graduate student. I would also like to thank Dr. Robert W. Birge for his guidance and encouragement. This experiment was proposed by Dr. John I. Shonle, who contributed very extensively during the initial planning of the experiment and during the Bevatron run.

The bubble chamber and its operating crew were provided by Professor Luis Alvarez's group, for which I am very grateful. Dr. Ronald Ross and Dr. William Humphrey provided the necessary information about the geometry and optical constants of the bubble chamber.

The Goldhaber group and the Ticho group constructed the separated pion beam. Dr. Theodore Stubbs was particularly helpful with the beam. The effort of all the members of the Powell-Birge group who helped to operate the beam is also gratefully acknowledged.

Dr. Edward J. Lofgren and his staff are thanked for the use of the Bevatron.

Layton Lynch did a great deal of the scanning. All of the measurers are thanked, in particular David Hupp, George Bole, David Fletcher and Robert Brosamer.

Howard White and his staff provided the data reduction. Shirley Buckman and Dennis Hall modified FOG to accomodate the 15-inch

Berkeley hydrogen bubble chamber. Loren Schalz carried out the many FAIR runs needed to analyse the data. The service provided by the many people in this group is greatly appreciated.

The countless hours of work at the scan table described in the section on Acceptance and Separation was done by Charlotte Scales. Miss Scales also did a great deal of work in bookkeeping, plotting graphs, etc. Her labors have contributed immeasurably to this experiment and are very much appreciated.

Conversations regarding the inelastic data with Dr. Zaven Guiragossian and Dr. Julius Solomon are gratefully acknowledged.

The manuscript was prepared by Nancy Wakeman, Marleigh Sheaf, George Bole and the Graphic Arts department.

My thanks also, to the many people at the Laboratory who are too numerous to be named, but without whose help this experiment would not have been possible.

This work was done under the auspices of the U. S. Atomic Energy Commission.

APPENDIX

For the scattering of spin zero and spin one-half particles, there is a non-spin-flip amplitude $f(\theta)$ and a spin-flip amplitude $g(\theta)$. The partial wave expansion of these is given by:[2]

$$f(\theta) = 1/k \sum_{\ell=0}^{\infty} \left[(\ell + 1)A_{\ell}^{+} + \ell A_{\ell}^{-} \right] P_{\ell} (\cos \theta)$$

and

$$g(\theta) = i/k \sum_{\ell=1}^{\infty} (A_{\ell}^{+} - A_{\ell}^{-}) P_{\ell}^{1} (\cos \theta)$$

where

$$A_{\ell}^{\pm} = \frac{e^{2i\delta_{\ell}^{J=\ell\pm 1/2}} - 1}{2i}$$

The δ_{ℓ}^{J} are the complex phase shifts. The differential cross section is given by:

$$\frac{d\sigma}{d\Omega} = \left| f \right|^2 + \left| g \right|^2$$

when the spin 1/2 particles are unpolarized.

Coulomb effects have been neglected. Also, since the π^+- p system is in a pure T = 3/2 state, the isotopic spin label has been suppressed.

Terminating the series at $\ell = 2$ gives:

$$f(\theta) = 1/k \left[A_0^{+} + (2A_1^{+} + A_1^{-}) \cos \theta + (3A_2^{+} + 2A_2^{-}) (3/2 \cos^2\theta - 1/2) \right]$$

and

$$g(\theta) = i/k \left[(A_1^{+} - A_1^{-}) + (A_2^{+} - A_2^{-}) 3\cos \theta \right] \sin \theta .$$

Then, substituting into the expression for the differential cross section, the coefficient of $\cos^4 \theta$ is:

$$1/k^2 \left\{ 9/4 \left| 3A_2^+ + 2A_2^- \right|^2 - 9 \left| A_2^+ - A_2^- \right|^2 \right\}$$

The minus sign multiplies the spin-flip contribution. Simplifying this expression further gives:

$$45/4k^2 \left\{ \left| A_2^+ \right|^2 + 4\mathrm{Re}A_2^- A_2^{+*} \right\} .$$

This expression can be negative only if both A_2^+ and A_2^- are non-zero and the phase difference between them is greater than $\pi/2$.

Therefore, at least D wave, and at least $J = 5/2$, must be present.

REFERENCES

1. H. A. Bethe and F. de Hoffmann, Mesons and Fields, Vol. 2: Mesons (Row, Peterson and Company, Evanston, Illinois, 1955), pp. 59-62.

2. J. Ashkin, Nuovo cimento Supp. 14, 221 (1959).

3. S. Bergia, F. Bonsignori, and A. Stanghellini, Nuovo cimento 16, 1073 (1960).

4. R. M. Sternheimer and S. J. Lindenbaum, Phys. Rev. 109, 1723 (1958). A complete list of references on this model is given in R. M. Sternheimer and S. J. Lindenbaum, ibid. 123, 333 (1961).

5. G. Goldhaber, S. Goldhaber, J. Kadyk, T. Stubbs, D. Stork, H. Ticho, Lawrence Radiation Laboratory Internal Report Bev-483, February 26, 1960 (unpublished). For a brief summary see T. Stubbs, H. Bradner, W. Chinowsky, G. Goldhaber, S. Goldhaber, W. Slater, D. Stork, and H. Ticho, Phys. Rev. Letters 7, 188 (1961).

6. Reference Manuals. FOG CLOUDY FAIR Bubble Chamber Data Processing System. Lawrence Radiation Laboratory Document UCID 1340 (unpublished).

7. J. P. Berge, F. T. Solomitz, and H. D. Taft, Rev. Sci. Instr. 32, pp. 538-543 (1961).

8. H. Cramer, Mathematical Methods of Statistics (Princeton University Press, Princeton, 1958) pp.233-236.

9. J. Brisson, J. Deteof, P. Falk-Vairant, L. van Rossum, G. Valladas, and L. Yuan, Phys. Rev. Letters 3, 561 (1959).

10. T. Devlin, B. Moyer, and V. Perez-Mendez, Phys. Rev. 125, 690 (1962).

11. R. Cool, O. Piccioni, and D. Clark, Phys. Rev. 103, 1082 (1956). A few points between 600 MeV and 1100 MeV were measured by H. C. Burrowes, D. O. Caldwell, D. H. Frisch, D. A. Hill, D. M. Ritson, R. A. Schluter, and M. A. Wahlig, Phys. Rev. Letters 2, 119 (1959).

12. J. A. Helland, T. J. Devlin, D. E. Hagge, M. J. Lango, B. J. Moyer, and C. D. Wood, 1962 International Conference on High Energy Physics at Cern, p. 3. These same authors have tabulated their data in detail in Lawrence Radiation Laboratory Report UCRL 10478, Sept. 1962 (unpublished).

13. R. E. von Holdt, PALSI — A Polynomial Approximating Code, Lawrence Radiation Laboratory Report UCRL-5504, March 1959 (unpublished).

14. E. L. Iloff, Interactions and Lifetimes of K Mesons, University of California, Lawrence Radiation Laboratory Report UCRL-3605, p. 43, Nov. 1956. (unpublished).

15. J. W. Cronin, Phys. Rev. 118, 824 (1960).

16. W. J. Willis, Phys. Rev. 116, 753 (1959).

17. R. Barloutaud, C. Choquet-Louedec, A Derem, J. Heughebaert, A. Leveque, and J. Meyer, Physics Letters 1, 207 (1962).

J. K. Kopp, A. M. Shapiro, and A. R. Erwin, Phys. Rev. 123, 301 (1961).

U. Bidan, F. Levy, N. Abbattista, A. Minafra, S. Mongelli, A. Romano, and P. Waloschek, Nuovo cimento 24, 334 (1962).

L. O. Roellig and D. A. Glaser, Phys. Rev. 116, 1001 (1959).

18. R. Barloutaud, C. Choquet-Louedec, A. Derem, J. Heughebaert, A. Leveque, and J. Meyer, Physics Letters 1, 207 (1962).

19. M. Horovitz and P. Yager, IBM Program ATHOS — Phase Space Calculations, Lawrence Radiation Laboratory Internal Report, Physics Note 394, May 1962. (unpublished).

20. D. L. Stonehill and H. L. Kraybill, Rev. Mod. Phys. 34, 503 (1962).

21. R. Barloutaud, L. Cardin, A. Derem, C. Gensollen, A. Leveque, C. Louedec, J. Meyer, and D. Tycko, Pion-Proton Interactions at 600, 800 and 900 MeV., CEN Saclay report (unpublished).

This report was prepared as an account of Government sponsored work. Neither the United States, nor the Commission, nor any person acting on behalf of the Commission:

A. Makes any warranty or representation, expressed or implied, with respect to the accuracy, completeness, or usefulness of the information contained in this report, or that the use of any information, apparatus, method, or process disclosed in this report may not infringe privately owned rights; or

B. Assumes any liabilities with respect to the use of, or for damages resulting from the use of any information, apparatus, method, or process disclosed in this report.

As used in the above, "person acting on behalf of the Commission" includes any employee or contractor of the Commission, or employee of such contractor, to the extent that such employee or contractor of the Commission, or employee of such contractor prepares, disseminates, or provides access to, any information pursuant to his employment or contract with the Commission, or his employment with such contractor.